Harnessing CRISPR interference to resensitize laboratory strains and clinical isolates to last resort antibiotics

Angelica Frusteri Chiacchiera, Michela Casanova, Massimo Bellato, Aurora Piazza, Roberta Migliavacca, Gregory Batt, Paolo Magni, Lorenzo Pasotti

scientific reports

Check for updates

OPEN

Harnessing CRISPR interference to resensitize laboratory strains and clinical isolates to last resort antibiotics

Angelica Frusteri Chiacchiera[1,2,3], Michela Casanova[1,2], Massimo Bellato[4], Aurora Piazza[5,6], Roberta Migliavacca[5,6], Gregory Batt[3], Paolo Magni[1,2,7] & Lorenzo Pasotti[1,2,3,7]✉

The global race against antimicrobial resistance requires novel antimicrobials that are not only effective in killing specific bacteria, but also minimize the emergence of new resistances. Recently, CRISPR/Cas-based antimicrobials were proposed to address killing specificity with encouraging results. However, the emergence of target sequence mutations triggered by Cas-cleavage was identified as an escape strategy, posing the risk of generating new antibiotic-resistance gene (ARG) variants. Here, we evaluated an antibiotic re-sensitization strategy based on CRISPR interference (CRISPRi), which inhibits gene expression without damaging target DNA. The resistance to four antibiotics, including last resort drugs, was significantly reduced by individual and multi-gene targeting of ARGs in low- to high-copy numbers in recombinant *E. coli*. Escaper analysis confirmed the absence of mutations in target sequence, corroborating the harmless role of CRISPRi in the selection of new resistances. *E. coli* clinical isolates carrying ARGs of severe clinical concern were then used to assess the robustness of CRISPRi under different growth conditions. Meropenem, colistin and cefotaxime susceptibility was successfully increased in terms of MIC (up to > 4-fold) and growth delay (up to 11 h) in a medium-dependent fashion. ARG repression also worked in a pathogenic strain grown in human urine, as a demonstration of CRISPRi-mediated re-sensitization in host-mimicking media. This study laid the foundations for further leveraging CRISPRi as antimicrobial agent or research tool to selectively repress ARGs and investigate resistance mechanisms.

Keywords Antimicrobial resistance, Antibiotic re-sensitization, CRISPR array, *Escherichia coli* clinical isolates, bla_{NDM}-type, bla_{ctx-M}-type, *mcr-1*

The rapid spread of multidrug resistant pathogens has become a global health concern, exacerbated by the lack of innovation in the pipelines for developing new antibiotics[1,2]. Alternatives to traditional antibiotic treatments are thus urgently needed to eradicate antimicrobial resistance (AMR)-associated infections and minimize the evolution of antibiotic-escape mechanisms. In recent years, CRISPR-based approaches have been proposed to develop both therapeutic agents acting as alternative or adjuvant to antibiotics[3–5], and molecular genetic tools for research purposes[6–13]. For instance, CRISPR antimicrobials have been designed by redirecting the cleavage of Cas nucleases towards chromosome-encoded or plasmid-borne antibiotic resistance genes (ARGs), resulting in cell death or antibiotic re-sensitization, respectively[14–17]. However, the practical use of CRISPR antimicrobial faces significant challenges, such as their efficient delivery into target bacteria and their potential inactivation by the immune system, the emergence of escaper cells, and the regulatory and ethical aspects related to the clinical application of this technology[18]. To counteract these limitations, advances have been made in the development of delivery vehicles[6,14–17,19–21], e.g., probiotics with conjugative plasmids optimized to reach almost 100% conjugation efficiency in the mouse gut[22]. Nonetheless, host range specificity and risk of incompatibility

[1]Department of Electrical, Computer and Biomedical Engineering, University of Pavia, Via Ferrata 5, Pavia, Italy. [2]Centre for Health Technologies, University of Pavia, Via Ferrata 5, Pavia, Italy. [3]Institut Pasteur, Inria, Université Paris Cité, 28 rue du Docteur Roux, Paris, France. [4]Department of Molecular Medicine, Department of Information Engineering, University of Padua, Via Gabelli 63, Padua 35121, Italy. [5]Department of Clinical-Surgical, Diagnostic and Pediatric Sciences, University of Pavia, Viale Brambilla 74, Pavia, Italy. [6]Fondazione IRCCS Policlinico San Matteo, Pavia, Italy. [7]These authors contributed equally: Paolo Magni and Lorenzo Pasotti. ✉email: lorenzo.pasotti@unipv.it

with resident plasmids still represent critical limitations[23]. Regarding the issue of resistance development, many studies showed that escape mutants can evade CRISPR targeting by mutations either in the CRISPR circuitry (Cas proteins and gRNA) or in the target gene[20,21,24–26], or due to the presence of anti-CRISPR (ACR) systems in the host genome[27]. Mutations can occur as a consequence of the SOS response triggered by Cas9-mediated double strand breaks, leading to an escape rate higher than the one considered as acceptable by the National Institute of Health[28]. In the AMR context, the risk of inducing mutations in target gene is of specific concern as it makes the new sequence immune to CRISPR targeting but it may still encode a functional protein, ultimately generating a new ARG variant. Focusing on overcoming mutations in target genes, a strategy based on the CRISPR *interference* (CRISPRi) technology could represent an attractive solution as it relies on the ability of dead-Cas9 (dCas9) to inhibit the expression of a desired gene without damaging the target DNA[29,30]. Re-sensitized cells are eventually killed upon antibiotic administration.

To date, the CRISPRi-based approach has been evaluated against ARGs located on the chromosome or low copy plasmids. Laboratory strains of *Escherichia coli* or *Mycobacterium smegmatis* have been re-sensitized to ampicillin, trimethoprim, sulfamethoxazole, rifampicin, erythromycin and tetracycline[21,31–33]. To our knowledge, only two studies addressed the CRISPRi-based antibiotic re-sensitization of clinical isolates, i.e., a methicillin-resistant *Staphylococcus aureus*[34] and two clinical strains of *Klebsiella pneumoniae* and *Escherichia coli* by targeting their ARGs[35].

Beyond the antimicrobial function, CRISPRi-based tools have been exploited to perform gene functional screenings for validating drug targets, dissecting AMR mechanisms and gaining insight into the consequences of partial gene inhibition in Mycobacterium and Acinetobacter[7,11–13,36]. Although the mentioned studies showed promising results, the potential of CRISPRi in both the design of antimicrobials and systems biology tools still needs to be improved by addressing the following challenges: inhibition of ARGs expressed from a high-copy plasmid (1); characterization of the repression efficiency of guide RNAs targeting CDSs rather than promoters, as transcriptional regulation regions may vary across strains (2); multi-targeting of genes located on different plasmids to assess the contribution of their respective copy numbers on CRISPRi re-sensitization (3); analysis of escaper cells to verify the absence of mutations in target genes (4); evaluation of CRISPRi robustness in different environments to quantify the impact of growth conditions on bacterial antibiotic response and CRISPRi-repression capability (5).

In light of these challenges, we first designed, tested and further optimized a CRISPRi-based platform in recombinant *E. coli* strains expressing four ARGs ($bla_{\text{TEM-116}}$, *tetA*, $bla_{\text{NDM-1}}$, *mcr-1*), by testing their single and multiple targeting. These ARGs were selected due to their different gene dosages (low- to high-copy plasmids), resistance mechanisms, and therapeutic relevance in clinical settings. Second, we analyzed escaper cells to study the bacterial response upon antibiotic re-exposure and to highlight the genetic mutations responsible for the rescue of surviving cells. Finally, to test our circuitry in clinically relevant case studies, we constructed a CRISPRi-based trans-conjugative platform to carry out a full delivery and re-sensitization workflow from engineered donors to four pathogenic *E. coli* strains: $bla_{\text{NDM-5}}$, *mcr-1*, $bla_{\text{ctx-M-14}}$ and $bla_{\text{ctx-M-15}}$ were individually repressed and their growth inhibition effects characterized in different growth media conditions.

Results

Repression of single and multiple ARGs in recombinant bacteria

The CRISPRi-mediated antibiotic re-sensitization was first assessed in recombinant *E. coli* strains. This preliminary investigation was conducted on *ad hoc* constructed case studies to test re-sensitization of strains with ARG in high-copy plasmid as well as the simultaneous inhibition of two ARGs. *tetA* or $bla_{TEM-116}$ were used as target ARGs. *tetA* is located on a very low copy F' episome (vLC, ~ 1.5 copies) and encodes for an efflux pump conferring resistance to tetracycline (TC); $bla_{TEM-116}$ is located on a high-copy vector (HC, ~ 70 copies) and encodes a broad-spectrum β-lactamase which provides resistance to many β-lactam antibiotics, including ampicillin (AMP). Such targets were selected due to their different resistance mechanisms and to evaluate CRISPRi efficiency against plasmids with different copy numbers. A set of three test strains was investigated: *sensitive* strain, without ARG-carrying plasmids; *resistant* strain, with the target ARG(s); *specific CRISPRi transformant* (henceforth *sCRISPRi*), bearing the ARG-carrying plasmid(s) and a CRISPRi platform targeting one or two ARGs (Supplementary Material Figure S1a). This set of strains was characterized via microplate and agar plate assays to quantify antibiotic re-sensitization in terms of minimum inhibitory concentration (MIC), growth delays (Δt) and inhibitory concentration killing at least 99% of the population (IC_{99}) (Supplementary Material Figure S1b, Tables S4 and S5).

Tetracycline re-sensitization in microplate assays by single ARG targeting. A two-plasmid CRISPRi platform targeting single ARGs has been adopted (Fig. 1a, Supplementary Material Figure S1a). The platform relied on a low-copy plasmid (LC, ~ 5 copies)[37], carrying the gRNA module under the control of an isopropyl-β-D-1-thiogalactopyranoside (IPTG)-inducible P_{LlacO1} promoter, and a medium-copy plasmid (MC, ~ 15 copies)[37,38], carrying the dCas9 module under the P_{J23116} weak constitutive promoter, previously evaluated as a high-repression efficiency and low-burden dCas9 expression cassette[39] (Fig. 1a). A gRNA module (gtetA) was designed to block *tetA* transcription by targeting its CDS. Representative growth profiles at different TC concentrations are reported in Fig. 1b for *resistant* and *sCRISPRi* strain and Supplementary Material Figure S2a for *sensitive* strain. We observed that the MIC of the *resistant* strain (MIC > 100 μg/ml) was more than 10-fold higher than that of the *sensitive* strain (MIC = 10 μg/ml); nonetheless, the growth of resistant cells started to be compromised for TC > 10 μg/ml, resulting in a delayed growth profile. On the other hand, *tetA* inhibition in the *sCRISPRi* strain contributed to a substantial increase in the time needed for population recovery in presence of sub-inhibitory TC concentrations, leading to a complete TC re-sensitization with a MIC of 100 μg/ml (Fig. 1b). The delayed growth of the *sCRISPRi* strain was interpreted as a response to *tetA* inhibition by dCas9:gtetA, drug sequestration (TetR could still reduce the concentration of free intracellular TC[40]) and possible loss of function

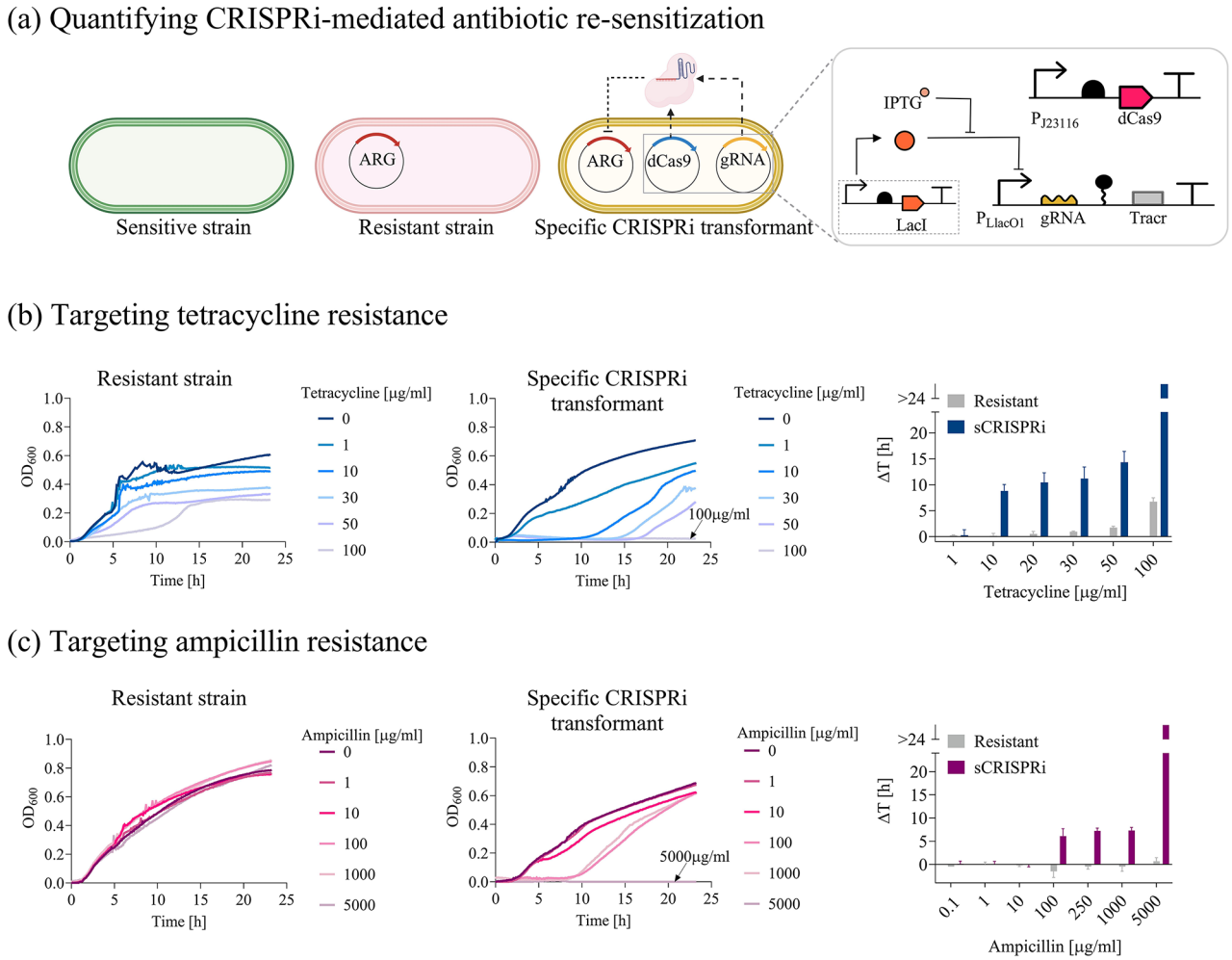

Fig. 1. Re-sensitization of laboratory strains to tetracycline and ampicillin by single ARG targeting. **(a)** Description of the test strains. The inhibition of *tetA* or $bla_{TEM-116}$ (red) is investigated with a two-plasmid CRISPRi platform, including a constitutive dCas9 module (blue) in a medium-copy plasmid and an IPTG-inducible sgRNA module (yellow) in a low-copy plasmid, transcribing gtetA, $gbla_{promoter}$ or $gbla_{CDS}$. Platform components are detailed in the inset according to the Synthetic Biology Open Language (SBOL) notation. **(b, c)** Growth profiles (subpanels on the left) and growth delays (subpanels on the right) of the *resistant* and *sCRISPRi* strains from microplate assays to investigate tetracycline (**b**) and ampicillin (**c**) re-sensitization. *sCRISPRi* strains are engineered with a CRISPRi platform, including constitutive dCas9 and IPTG-inducible gtetA or $gbla_{promoter}$ targeting *tetA* or $bla_{TEM-116}$, respectively. The overlapped curves in which a complete growth inhibition was achieved are indicated with an arrow, with the list of the corresponding antibiotic concentrations. Representative curves are shown from a set of at least three independent experiments. Growth delays (Δt) of treated strains are relative to the growth profile without antibiotics for the *resistant* and *sCRISPRi* strains. Bars represent means and standard deviations (N = 3). The bars over the interrupted axis indicate the antibiotic concentration (MIC) for which OD_{600} was lower than 0.1. Data come from experiments in LB media in the presence of IPTG. TOP10 F' and T-cr_{sgT_const} were used as *resistant* and *sCRISPRi* strains, respectively, to investigate tetracycline re-sensitization. A-res and A-cr_{sgA_const} were used as *resistant* and *sCRISPRi* strains, respectively, to investigate ampicillin re-sensitization.

mutations occurring in the CRISPRi circuitry. The delays in *sCRISPRi* strain recovery increased as a function of TC concentration, with significantly larger delay values than the *resistant* strain ($p < 0.05$, t-test) (Fig. 1b). The *sCRISPRi* strain tested in the absence of IPTG indicated that the leakiness of P_{LlacO1} activity was sufficient to restore TC susceptibility, as a low amount of the dCas9:gtetA repressor complex was already effective in inhibiting *tetA* expressed from a vLC plasmid with no relevant difference from the on-state (Supplementary Material Figure S3a, c).

Ampicillin re-sensitization in microplate assays by single ARG targeting. The same CRISPRi platform described in Fig. 1a was used to test $bla_{TEM-116}$ inhibition. Two gRNAs ($gbla_{promoter}$ and $gbla_{CDS}$) were designed to prevent or block $bla_{TEM-116}$ transcription by targeting its promoter or CDS, respectively (Fig. 1c, Supplementary Material Figure S4). We observed that the *resistant* strain was able to withstand even the highest AMP concentration tested, without relevant growth defects, resulting in a MIC > 5000 µg/ml (Fig. 1c), which was much higher than that of

the *sensitive* strain (MIC = 10 μg/ml) (Supplementary Material Figure S2b). In the *sCRISPRi* strain, $bla_{TEM-116}$ inhibition by a gRNA targeting *bla* promoter led to a MIC of 5000 μg/ml and a growth delay of 6–7 h for AMP between 10 and 1000 μg/ml (Fig. 1c). Targeting the *bla* CDS instead of its promoter had a weaker effect, since a complete growth inhibition was not observed for the antibiotic concentrations tested. A higher growth delay than the resistant control was detected only for AMP > 250 μg/ml ($p < 0.05$, t-test), reaching a 7-h delay only for AMP = 5000 μg/ml (Supplementary Material Figure S4). These data confirm that the location of the target site can strongly affect repression efficiency, as previously described[29]. As expected, growth profiles in the absence of IPTG showed that in the context of ARG in HC plasmid the repression performance was lower than in a vLC plasmid, tested above, as the leakage of P_{LlacO1} led to a slightly delayed growth (2.5 h) only for the highest AMP concentration ($p < 0.05$, t-test) (Supplementary Material Figure S4). Here, different mechanisms can contribute to the growth delays, including $bla_{TEM-116}$ repression, occurrence of mutations inactivating CRISPRi circuitry or emergence of collective antibiotic tolerance[41].

Another set of TC- and AMP-resistant control strains, bearing a full CRISPRi plasmid set with non-specific sgRNA (*nsCRISPRi* with $gbla_{CDS}$ and gtetA, respectively), was evaluated, yielding similar delay patterns to the *resistant* strains described above (Supplementary Material Figure S5). This demonstrates the specificity of our system and also that the two CRISPRi plasmids used in this section did not cause relevant burden to the engineered cells.

Finally, escaper cells recovered from the highest AMP and TC concentration were used to perform a second round of antibiotic treatment. We observed comparable growth profiles with the *resistant* strain (Supplementary Material Figure S6), suggesting that a population of mutants with increased MIC was selected over the 24 h time course.

Tetracycline and ampicillin re-sensitization in agar plate assays by single ARG targeting. To test whether the growth in liquid or solid media could affect the rescue of escaper cells, we performed agar plate assays (Supplementary Material Figures S1, S7, and Table S4). We expected different results from liquid cultures in which an enrichment of escapers can occur due to the activity of enzymes degrading the antibiotic in the media (i.e., β-lactamases released by lysed cells allow population recovery via a phenomenon known as collective antibiotic tolerance[41]). This response is likely to be mitigated for isolated colonies on agar plates. Data of TC and AMP agar plate assays were qualitatively consistent with the data in microplate assays (Supplementary Material Figure S7 and Table S4): *sCRISPRi* strains (*sCRISPRi-sgRNA* in the figure) exhibited lower IC_{99} values (TC = 5 μg/ml, AMP = 50 μg/ml) than *resistant* strains (TC = 50 μg/ml, AMP > 1000 μg/ml), resulting in a 10-fold and > 20-fold increase of antibiotic susceptibility for TC and AMP, respectively. Consistent with microplate assays, the $gbla_{CDS}$ strain exhibited a higher IC_{99} (150 μg/ml) than the $gbla_{promoter}$ strain, still representing a relevant improvement in growth inhibition (> 6-fold susceptibility compared with *resistant* strain).

These data confirm that our CRISPRi platform can effectively inhibit single ARGs in low but also HC plasmids, leading to increased sensitivity to the respective antibiotics in recombinant *E. coli*.

Multi-targeting of ARGs using a constitutive dCas9. The platform described above was extended to address the simultaneous targeting of *tetA* and $bla_{TEM-116}$. The individual sgRNA cassette was replaced with two guide RNA architectures: double sgRNA cassette or CRISPRi array[42–44]. Both of them enable the simultaneous transcription of gtetA and $gbla_{promoter}$ under the control of the same regulatory elements (IPTG-inducible P_{LlacO1} promoter and synthetic terminator) (Fig. 2a). The transcription of dCas9 protein was kept under the control of the P_{J23116} weak constitutive promoter, to eventually investigate the effect of dCas9 sharing between different guides on their multi-targeting capability (Fig. 2a). The resulting *sCRISPRi* strains harbored a two-plasmid CRISPRi platform and two different ARG-carrying plasmids (Supplementary Material Figure S1a, Table S1). The described platform showed a lower performance than the individual gRNA cassette tested above, as MICs could not be determined in liquid assays (Fig. 2b, d, and Supplementary Material Figure S8). The decrease in repression efficiency was interpreted as the result of gRNAs competition for the shared pool of dCas9 protein, which ultimately affects the number of repressor complexes that can bind and inhibit target genes[45,46].

Multi-targeting of ARGs using an inducible dCas9. To overcome the competition between gRNAs, an N-3-oxohexanoyl-L-homoserine lactone (HSL)-inducible dCas9 module was placed in the same plasmid already hosting the double sgRNA cassette or CRISPRi array, leading to the transition to a one-plasmid CRISPRi platform (Fig. 2a, Supplementary Material Figure S1a). TC and AMP growth inhibition assays were performed with a range of HSL concentrations to find an optimal dCas9 expression level, which was determined based on the analysis of growth delays (Supplementary Material Figure S9). Regarding TC-treatment, a full susceptibility was restored in the HSL-inducible dCas9 strain at the same MIC as the single sgRNA cassette (MIC = 100 μg/ml). Regarding AMP treatment, a major improvement over the previous platform is evidenced by the significantly increased delay in growth recovery at AMP concentrations higher than 250 μg/ml ($p < 0.05$, t-test) (Fig. 2c, d). Data from agar plate assays showed a consistent pattern (Supplementary Material Figure S7): the one-plasmid inducible circuit displayed the same re-sensitization efficiency to TC as the single sgRNA cassette (IC_{99} = 5 μg/ml); for AMP, a 4-fold increase of IC_{99} (200 μg/ml) was observed compared to that of the *sCRISPRi* strain bearing a single sgRNA cassette (50 μg/ml), confirming the impact of guide RNA competition on the silencing performances of a high copy number target gene. Overall, data showed that dCas9 tuning contributed to increase both TC- and AMP-sensitivity, although it was not sufficient to fully counteract gRNAs competition for HC-targets. Finally, the two gRNAs architectures were compared based on the analysis of growth delays at the fixed HSL concentration. Due to its better performance, the inducible dCas9 with CRISPRi array design was selected for subsequent analyses (Supplementary Material Figure S9). This double targeting system also enabled to increase the recovery time of laboratory strains bearing both $bla_{TEM-116}$ and *tetA* in a combined treatment with AMP and TET (Supplementary Material Figure S10).

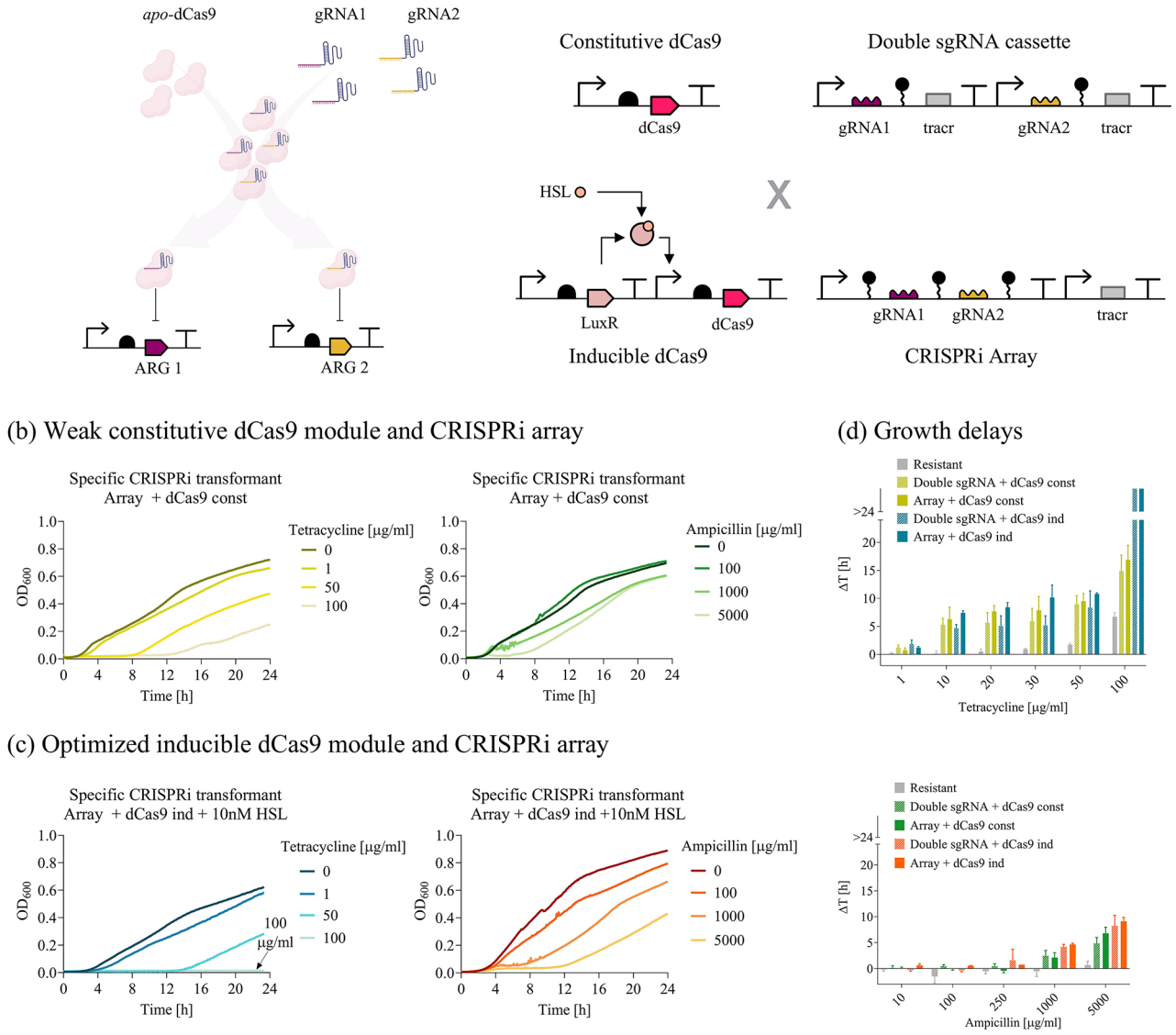

Fig. 2. Re-sensitization of laboratory strains to tetracycline and ampicillin by multiple ARG targeting. **(a)** Illustration of multiplexed targeting of tetracycline and ampicillin resistance genes by two guides repressing *tetA* and $bla_{TEM-116}$. Description of all the synthetic circuit combinations tested with two guide RNAs: weak constitutive or N-3-oxohexanoyl-L-homoserine lactone (HSL)-inducible dCas9, and IPTG-inducible CRISPRi array or sgRNA tandem cassettes (double sgRNA cassette), yielding four different circuit designs. **(b, c)** Growth profiles of *sCRISPRi* strains from microplate assays to investigate tetracycline (left subpanel) and ampicillin (right subpanel) re-sensitization. *sCRISPRi* strains are engineered with a two-plasmid CRISPRi platform, including constitutive dCas9 and IPTG-inducible CRISPRi array transcribing gtetA and $gbla_{promoter}$ simultaneously (panel **b**). *sCRISPRi* strains are engineered with a one-plasmid CRISPRi platform, including HSL-inducible dCas9 (HSL concentration was set to 10 nM) and IPTG-inducible CRISPRi array transcribing gtetA and $gbla_{promoter}$ simultaneously (panel **c**). Representative curves are shown in (**b, c**) from a set of at least three independent experiments. **(d)** Growth delays (Δt) of treated strains relative to the growth profile without antibiotics for the *resistant* strain and the four *sCRISPRi* strains with two-guide architectures. Bars represent means and standard deviations ($N=3$). The bars over the interrupted axis indicate the antibiotic concentration (MIC) for which OD_{600} was lower than 0.1. All the data come from experiments in LB media in the presence of IPTG and HSL. AT-cr_{sgAT_const} and AT-cr_{arAT_const} were used as *sCRISPRi* strains with constitutive dCas9 and inducible double sgRNA cassette or CRISPRi array, respectively. AT-cr_{sgAT} and AT-cr_{arAT} were used as *sCRISPRi* strains with inducible dCas9 and inducible double sgRNA cassette or CRISPRi array, respectively.

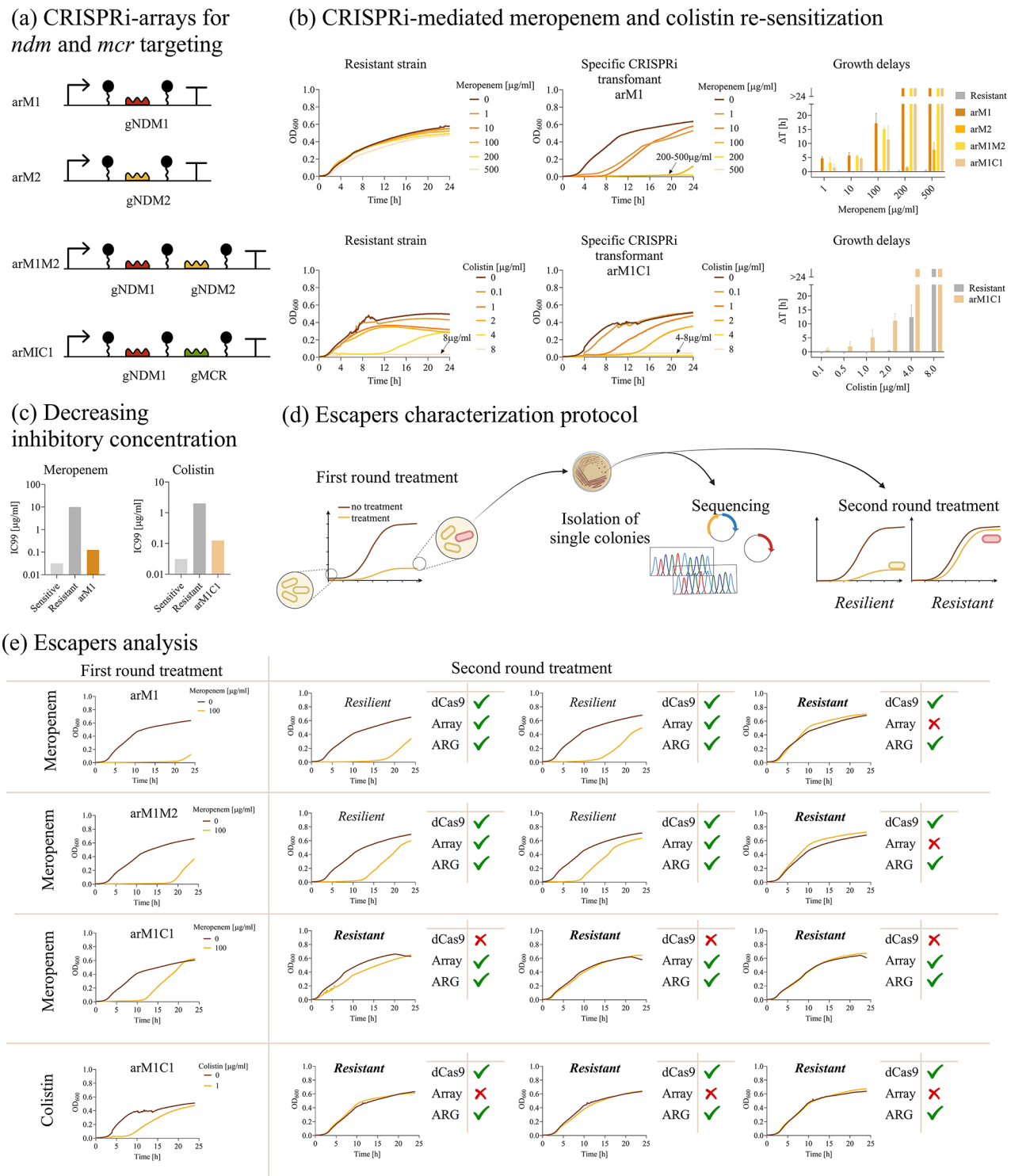

Sensitization of engineered bacteria to last-resort antibiotics

We reprogrammed the one-plasmid system with CRISPRi array described in Fig. 2a to inhibit the expression of two clinically relevant ARGs, bla_{NDM} and *mcr*, conferring resistance to meropenem (MER) and colistin (COL), respectively. Both antibiotics are classified as last-resort drugs, representing an example of the few remaining therapeutic options available to treat severe AMR-associated infections. A set of four CRISPRi arrays was designed to target conserved positions among bla_{NDM} and *mcr* variants (Fig. 3a and Supplementary Material Figure S11). In particular, the inhibition of bla_{NDM} was characterized with two gRNAs (gNDM1 and gNDM2) included as single- (arM1, arM2) or double-spacers (arM1M2) in the CRISPRi array. The comparison between individual and combined spacers against bla_{NDM} was investigated to determine whether increasing the number of target sequences could enhance repression efficiency and/or limit escape mutations. The efficiency of a fourth array carrying a non-targeting gRNA (arM1C1) was also characterized for bla_{NDM} inhibition. The same array was used to test the inhibition of *mcr* with one gRNA (gMCR) (Fig. 3a). MC vectors were transformed in *resistant* and

◀**Fig. 3**. Re-sensitization of laboratory strains to last-resort antibiotics by single and multiple ARG targeting. **(a)** Description of CRISPRi arrays transcribing single or double spacers for bla_{NDM-1} and/or *mcr-1* targeting, with names provided on the left. **(b)** Growth profiles of *resistant* and *sCRISPRi* strains from microplate assays to investigate meropenem (top) and colistin (bottom) re-sensitization. *sCRISPRi* strains are engineered with a one-plasmid CRISPRi platform, including HSL-inducible dCas9 and IPTG-inducible CRISPRi arrays targeting bla_{NDM-1} (arM1) or *mcr-1* (arM1C1) gene. The overlapped curves in which a complete growth inhibition was achieved are indicated with an arrow, with the list of the corresponding antibiotic concentrations. Representative curves are shown from a set of at least three independent experiments. Growth delays (Δt) of treated strains relative to the growth profile without antibiotics for the *resistant* and *sCRISPRi* strains (four for meropenem assays and one for colistin assays), corresponding to the guide RNA designs of panel (**a**). Bars represent means and standard deviations (N = 3). The bars over the interrupted axis indicate the antibiotic concentration (MIC) for which OD_{600} was lower than 0.1. **(c)** Antibiotic concentrations inhibiting bacterial growth by at least 99% (IC_{99}) in agar plate assays. IC_{99} values for meropenem and colistin are shown for the strain with HSL-inducible dCas9 (induced with 10 nM HSL) and the arM1 and arM1C1 CRISPRi arrays, respectively. Bars represent the antibiotic concentrations in at least two independent experiments that provided consistent values, therefore no error bars are present. **(d)** Illustration of the experimental setup used to study escaper populations that showed recovery after antibiotic treatment in microplate assays. Supernatants of three *sCRISPRi* strains were also assayed to qualitatively investigate the antibiotic concentration remaining at the end of the experiment (Supplementary Material Figure S17). **(e)** Analysis of escaper strains in four different conditions: arM1, arM1M2 and arM1C1 with meropenem treatment, and arM1C1 with colistin treatment. Representative curves without antibiotics and with a sub-lethal antibiotic concentration are shown for a microplate assay (first round). Three growth profiles are shown for single colonies of the escapers isolated from the treated culture of the first round and assayed as above (second round), each classified with a phenotype (resistant or resilient). Sequencing statistics are shown for each escaper, with ticks and crosses indicating correct and mutated sequences, respectively, for dCas9, CRISPRi array, and ARG. All the data come from experiments in LB media in the presence of IPTG and HSL. TOP10 F', M-res, M-cr_{arM1}/M-cr_{arM2}/M-cr_{arM1M2}/M-cr_{arM1C1} were used as *sensitive*, *resistant* and *sCRISPRi* strains, respectively, to investigate meropenem re-sensitization. TOP10 F', C-res and C-cr_{arM1C1} were used as *sensitive*, *resistant* and *sCRISPRi* strains, respectively, to investigate colistin re-sensitization.

sCRISPRi strains to express the ARGs (pGDP1 NDM-1 or pGDP2 MCR-1, bearing an *E. coli* codon-optimized bla_{NDM-1} driven by the P_{bla} promoter, and an *mcr-1* gene driven by the P_{lac} promoter)[47] (Fig. 3a).

Microplate assays for meropenem re-sensitization in laboratory strains. First, we examined the antibiotic response in the six strains for investigating bla_{NDM-1} inhibition (four *sCRISPRi* strains with gNDM1, gNDM2, gNDM1-gNDM2, gNDM1-gMCR1, and their *sensitive* and *resistant* controls). Growth delays and representative growth profiles at different MER concentrations are reported in Fig. 3b and Supplementary Material Figure S12. We observed that the *resistant* strain was able to withstand even the highest MER concentration tested, without relevant growth defects, resulting in a MIC > 500 μg/ml, which was more than 500-fold higher than the one of the *sensitive* strain (MIC < 1 μg/ml). In the gNDM-1 *sCRISPRi* strain, a significant growth delay is already evident for the lowest MER concentration (1 μg/ml). High delay values (up to 17 h) are reached for MER = 100 μg/ml, with MIC determined at 200 μg/ml (Fig. 3b). Conversely, gNDM2 caused a growth delay up to about 8 h only for much higher antibiotic concentrations (MER = 500 μg/ml) with no complete growth inhibition, and statistically significant delay values only for MER > 100 μg/ml (Fig. 3b). This result was consistent with the previously described data on the $bla_{TEM-116}$ CDS repression (Supplementary Material Figure S4). The use of the gNDM1-gNDM2 array showed similar results to the strain with gNDM1 only, suggesting that an additional guide RNA did not improve silencing efficiency. Regarding gNDM1-gMCR1, we observed only a slight decrease in efficiency, while growth delay values comparable to gNDM1 and gNDM1-gNDM2 (less than 1.5-fold difference) and the same MIC (200 μg/ml) were determined (Fig. 3b); a statistical comparison among the data of gNDM1, gNDM1-gNDM2 and gNDM1-gMCR1 for each MER concentration demonstrated that the system was not significantly affected by competition with a second spacer targeting another sequence ($p > 0.05$, ANOVA).

The same experimental design was adopted to quantify bla_{NDM-1} inhibition in MG1655, to extend the characterization of CRISPRi re-sensitization to a K-12 model strain and enable a comparison with the TOP10 F' background (Supplementary Material Figure S13). MG1655 showed the same MIC values as TOP10 F' for the *sensitive* (MER < 1 μg/ml) and *nsCRISPRi* (MER > 500 μg/ml) controls. For *sCRISPRi* strains with the gNDM1, gNDM1-gNDM2 and gNDM1-gMCR1 arrays, we observed meropenem re-sensitization at MIC = 500 μg/ml, while gNDM2 confirmed its poor functionality. Growth delays were significantly higher than the non-specific control for sub-inhibitory MER concentrations and confirmed the absence of competition effects caused by a second spacer in the array. The difference between MIC values in re-sensitized MG1655 and TOP10 F' (500 vs. 200 μg/ml) may depend on several factors, e.g., different growth rates or dCas9/array expression levels between strains. This underscores the impact of the strain genetic background on the antibiotic resistance response, although our CRISPRi system successfully confirmed its functionality in a different host.

Together, the data on TC, AMP and MER re-sensitization showed that our one-plasmid CRISPRi platform with inducible dCas9 resulted in similar performance between individual guide RNA and two-spacer systems when targeting ARGs present in vLC and MC plasmids. This encourages the use of two-spacer CRISPRi arrays potentially targeting multiple resistance genes.

Microplate assays for colistin re-sensitization in laboratory strains. Then, we examined antibiotic response in the three strains for investigating COL resistance repression (Fig. 3b and Supplementary Material Figure S14). We observed that the growth of the *resistant* strain was almost unaffected up to COL = 2 μg/ml, and the final MIC determined (8 μg/ml) was 8-fold higher than that of the *sensitive* strain. In the gMCR1 *sCRISPRi* strain, we determined a 2-fold lower MIC than that of *resistant* strain (Fig. 3b). Moreover, comparing the growth profiles and growth delays of *sCRISPRi* and *resistant* strains, the effect of CRISPRi silencing resulted in a gradual increase of growth delay for sub-lethal COL levels, with values that were systematically higher and statistically different from the *resistant* strain at the 1 and 2 μg/ml antibiotic concentrations ($p < 0.05$, t-test). As in the case of meropenem, *mcr* inhibition was also assessed in a K-12 model strain (Supplementary Material Figure S15). MG1655 showed the same MIC value as TOP10 F' for the *sensitive* strain (COL = 1 μg/ml). However, different from TOP10 F', no MIC could be determined for the *nsCRISPRi* control (COL > 8 μg/ml). *sCRISPRi* with the gNDM1-gMCR1 array showed that the growth of MG1655 could also be efficiently inhibited with a MIC of 8 μg/ml and higher growth delay values than the resistant control, further confirming the conclusions obtained for the TOP10 F' laboratory strain.

Overall, these data showed a clear effect on colistin re-sensitization even using only one gRNA integrated in a double-spacer CRISPRi array.

Agar plate assays for confirming re-sensitization to meropenem and colistin. The IC_{99} values of *ndm-* and *mcr-sCRISPRi* strains in the TOP10 F' host (0.125 μg/ml of MER and COL) were 80- and 16-fold lower than those of *resistant* controls (MER = 10 μg/ml and COL = 2 μg/ml) (Fig. 3c). Moreover, these values approached the IC_{99} of the *sensitive* strain, showing only 4-fold difference (Supplementary Material Table S4).

Analysis of escapers to meropenem and colistin administration. Single colonies of *sCRISPRi* TOP10 F' strains recovered from one of the highest MER and COL concentrations in microplate assays were collected from three independent experiments and analyzed in a second round of treatment to gain insight into the adaptation factors supporting their regrowth (Fig. 3d). Indeed, the comparison of growth profiles after first and second round treatment enables the discrimination between a resistant phenotype (similar to *resistant* strain) or resilient phenotype (similar to *sCRISPRi* strain)[41]. We first studied MER-escapers and we observed both resilient and resistant phenotypes after exposure to MER (Fig. 3e, Supplementary Material Figure S16), suggesting the presence of heterogeneous populations evolving through community and adaptive antibiotic responses. Consistent with these data, the concentration of MER in the supernatant of recovered strains was lower than in the culture of a *sensitive* strain, probably due to antibiotic degradation by secreted β-lactamase, from both mutated and resilient cells, and supporting a permissive environment for resilient escapers (Supplementary Material Figure S17). Conversely, the delay pattern of gMCR1 *sCRISPRi* strain always resembled that of *resistant* control, as highlighted by the decreased delay in growth recovery and the increased MIC value, suggesting the selection of a population of resistant escapers (Fig. 3e and Supplementary Material Figure S16). Sequencing and restriction mapping on plasmid DNA revealed the absence of mutations in resilient cells, while inactivating mutations were found in resistant cells within the CRISPRi array (deletion of one or both spacers, 5 strains) or the dCas9 gene (insertion sequence, 3 strains). Importantly, no mutation was detected in ARG sequences, as well as no relevant copy number variation for the ARG-carrying plasmid (evaluated by electrophoresis gel analysis).

These data indicated that CRISPRi devices can re-sensitize recombinant *E. coli* strains against clinically-relevant antibiotics, although escapers with an inactivated CRISPRi system still occur at sub-lethal MER- and COL-concentrations.

Horizontal transfer of CRISPRi repression devices in clinical isolates

We tested our CRISPRi platform in *E. coli* clinical isolates to evaluate its use for clinically relevant applications[48–50]. Notably, clinical isolates can harbor a vast collection of ARGs and genomic mutations that cooperate to generate high-level resistance[51]. In addition, the low transformation efficiency of non-model bacteria may hinder their engineering with synthetic circuits[52]. To address CRISPRi delivery, we adopted a trans-conjugative platform consisting of pTA-Mob helper plasmid, bearing the RK2 conjugative machinery[53], and a mobilizable vector, carrying the CRISPRi circuitry and an origin of transfer (oriT from pRK2) (Supplementary Material Figure S18a).

Platform functioning was first assessed on the previously investigated AMP-, MER- and COL-resistant laboratory strains to measure conjugation frequency and the percentage of transconjugants re-sensitized to a target antibiotic. After 24 h mating with recipients carrying $bla_{TEM-116}$, bla_{NDM-1} or *mcr-1* gene, we determined a conjugation frequency ranging from $9*10^{-5}$ to $2*10^{-2}$ (Supplementary Material Figure S18b), consistent with the values reported in the literature[20]. We then quantified the proportion of AMP-, MER- and COL-resistant transconjugants effectively re-sensitized to the respective target antibiotic, and we found that it ranged from 71 to 99.9% (Supplementary Material Figure S18c).

On the one hand, these data confirmed that the conjugative transfer of CRISPRi circuits targeting three different ARGs can effectively restore the susceptibility to a fixed antibiotic concentration in almost all the population of engineered bacteria that received the mobilized plasmid; on the other hand, the low efficiency of the conjugative transfer still remains a limit of this approach, as acknowledged in the literature[18].

Re-sensitization of meropenem-, colistin- and cefotaxime-resistant clinical isolates. Two *E. coli* strains expressing bla_{NDM-5} or *mcr-1* genes were first adopted to investigate the ability of CRISPRi to increase susceptibility to the same target antibiotics as in the previous section, i.e., MER and COL. The MER-resistant isolate is a high-risk multiresistant ST167 clone collected from a liver sample of a kitten[49]. This isolate is of particular concern due to the presence of several antibiotic resistance genes, including multiple β-lactamase determinants like bla_{ble}, bla_{AmpH}, bla_{AmpC1}. The clinical relevance of this strain is reinforced by the previously demonstrated transmission of an ST167 NDM-5-producing *E. coli* between animals and humans[54]. The COL-resistant isolate is an ST617 clone recovered from a patient admitted to the rehabilitation ward of a hospital in Northern Italy[48]. For each

recipient strain, conjugations were carried out to generate transconjugants bearing a specific CRISPRi array (henceforth *sCRISPRi*^{trans}) targeting *bla*$_{NDM-5}$ or *mcr-1* gene, and transconjugants bearing a non-specific CRISPRi array (henceforth *nsCRISPRi*^{trans}) used as control strains.

Using the engineered strains obtained by conjugation, growth inhibition assays were performed in Mueller Hinton (MH) broth, a nutrient-rich medium recommended by EUCAST and CLSI for antibiotic susceptibility testing. Results of microplate assays over 24 h time courses revealed that the susceptibility to both MER and COL was successfully increased in *sCRISPRi*^{trans} strains, exhibiting a > 4- and 2-fold lower MIC than that of control strains, respectively (Fig. 4b-c and Supplementary Material Table S6). Moreover, we performed MH agar plate assays and we observed that the concentration of surviving transconjugants decreased up to 163- and 4-fold for MER = 1 μg/ml and COL = 0.25 μg/ml, respectively (Supplementary Material Figure S19).

To further evaluate the potential of our platform in different clinical isolates and with a different antibiotic, we investigated the cefotaxime re-sensitization in two *E. coli* strains expressing the *bla*$_{ctx-M-14}$ and *bla*$_{ctx-M-15}$ genes. CTX-M enzymes represent a group of extended-spectrum β-lactamases (ESBLs) disseminated worldwide, with CTX-M-14 and CTX-M-15 being the most prevalent variants in gram-negative pathogens[55,56]. The two clinical isolates (NILS18 and NILS56) are part of the Natural Isolates with Low Subcultures (NILS) pathogenic *E. coli* collection[50], and were collected from blood (*bla*$_{ctx-M-14}$ strain) and urine (*bla*$_{ctx-M-15}$ strain) samples, respectively. It is worth noting that, in addition to the *bla*$_{ctx-M-14}$ gene, the same strain carries *bla*$_{TEM-1B}$ which contributes to provide resistance to β-lactam antibiotics.

A new set of CRISPRi arrays carrying a single spacer, gCTX-M-14 or gCTX-M-15, was designed to individually target the respective ARGs and used to engineer the two CTX-resistant strains by conjugation (Fig. 4a). Results of 24 h time courses with *bla*$_{ctx-M-14}$ transconjugants showed that the growth of the *nsCRISPRi* control was not inhibited at any of the tested CTX concentrations, while a MIC was observed for the *sCRISPRi*^{trans} (256 μg/ml), suggesting that the CRISPRi inhibition of *bla*$_{ctx-M-14}$ can increase by > 2-fold the sensitivity to cefotaxime in MH (Fig. 4d and Supplementary Material Table S6). Consistent with these observations, a significant difference was found in the growth delays of both strains at sub-lethal CTX levels ($p < 0.05$, t-test), with differences up to 3.5 h (Fig. 4d). On the other hand, none of the CTX concentrations tested resulted in a complete growth inhibition over 24 h for *bla*$_{ctx-M-15}$ strains, thus preventing MIC determination (Fig. 4e and Supplementary Material Table S6). However, the effect of CRISPRi on *bla*$_{ctx-M-15}$ inhibition was still highlighted by a significant increase of growth delay values from *nsCRISPRi*^{trans} to *sCRISPRi*^{trans}, with statistically significant differences for nearly all the CTX concentrations tested ($p < 0.05$, t-test) (Fig. 4e).

The reported MICs in microplate assays were determined by 24 h time courses in which the temporal dynamics of strains in response to different antibiotics was observed. In addition, we performed antimicrobial susceptibility testing according to EUCAST guidelines, to determine EUCAST MICs via standard protocols (Supplementary Material Table S6) and enable comparisons with clinical breakpoints. Inhibition of *bla*$_{NDM-5}$ and *mcr-1* in the *sCRISPRi*^{trans} strains resulted in 4- and 2-fold lower EUCAST MICs than the respective *nsCRISPRi*^{trans} controls, while the inhibition of *bla*$_{ctx-M-14}$ and *bla*$_{ctx-M-15}$ resulted in no detectable EUCAST MICs up to 512 μg/ml of CTX. Comparing the EUCAST MICs with the MICs from microplate assays, the *mcr-1* and *bla*$_{ctx-M-15}$ strains showed consistent values. Conversely, the *bla*$_{NDM-5}$ and *bla*$_{ctx-M-14}$ *sCRISPRi*^{trans} strains showed a higher value for EUCAST MIC. According to EUCAST breakpoint designations, the four clinical strains bearing ARG-inhibition platforms were still classified as resistant, probably because of their very high resistance levels and additional genes/mutations that may work together with the target ARGs to increase resistance. Even applying two protocols that differ in the experimental setup, we further confirmed the functioning of our platform, with the only exception of the *bla*$_{ctx-M-14}$ *sCRISPRi*^{trans} strain which showed a detectable MIC in microplate assays but not with EUCAST protocol.

Re-sensitization of meropenem-, colistin- and cefotaxime-resistant clinical isolates in LB and M9 media. Antibiotic-resistant bacteria can colonize different environments in which they adapt their growth based on available resources. Given this aspect, we tested whether the repression capability of our platform was robust under different experimental conditions affecting the growth of CRISPRi strains. In particular, we performed growth inhibition assays in rich and poor media to evaluate how the composition of these media affected the resistance profile of target strains and, accordingly, the CRISPRi repression capability. Indeed, the role played by nutrient composition in modulating bacterial regrowth kinetics and antibiotic susceptibility was previously shown[57].

MER-, COL- and CTX-microplate assays were therefore performed in two standard growth media: minimal M9 medium with 0.1% lactose, selected as a nutrient-poor media based on inorganic salts and a carbon source, and the complex LB medium, used for assaying laboratory strains throughout this work and based on amino acids as main carbon sources, like MH (Fig. 5, Supplementary Material Figure S20).

Considering the growth profiles of all the strains in the three tested media (MH, M9, LB), a first major effect was a systematic increase in the antibiotic sensitivity of both non-specific and specific CRISPRi transconjugants grown in M9, in which the MIC values decreased up to 16-fold compared with those observed in MH or LB media (Figs. 4 and 5).

Considering the *bla*$_{NDM-5}$ *nsCRISPRi*^{trans} strain, all the MER concentrations tested (up to 32 μg/ml) supported growth in both MH and LB media (Figs. 4b and 5a). A MIC of 8 μg/ml was determined in M9, representing a > 4-fold higher sensitivity than in rich media (Fig. 5b). Similarly, the MIC of *sCRISPRi*^{trans} grown in M9 (MIC = 2 μg/ml) was 4- and 8-fold lower than those determined in MH (MIC = 8 μg/ml) and LB (MIC = 16 μg/ml), respectively (Figs. 4b and 5a, b).

A comparison of MIC values between *nsCRISPRi*^{trans} and *sCRISPRi*^{trans} showed significant changes between *bla*$_{NDM-5}$-strains in each tested media: the highest value was achieved in MH (FC > 4), followed by M9 (FC = 4) and LB (FC > 2) (Figs. 4b and 5a, b). The contribution of the CRISPRi system also impacted antibiotic susceptibility at sub-lethal MER concentrations in terms of growth delays. Data showed that *bla*$_{NDM-5}$ inhibition

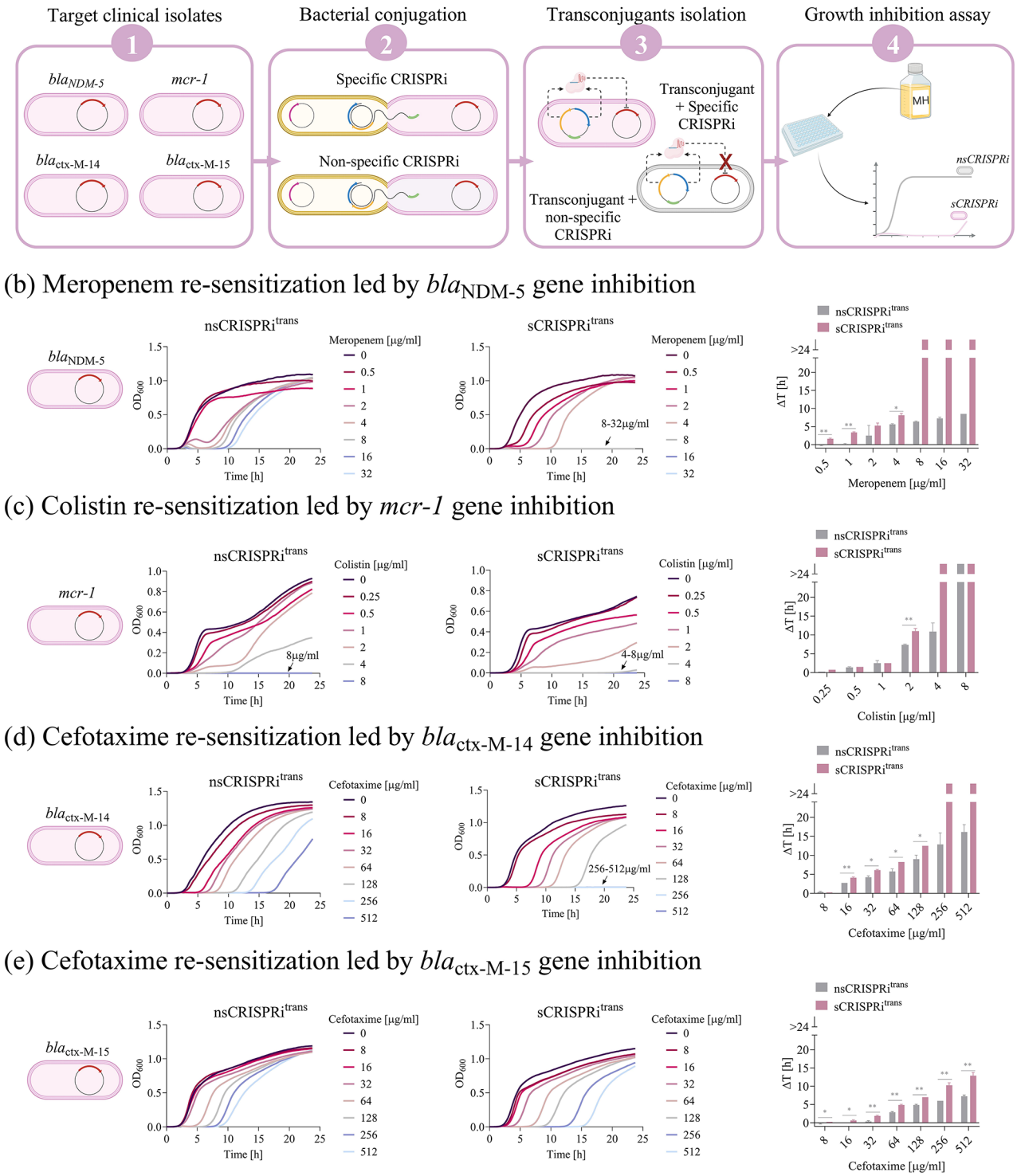

in *sCRISPRi*^{trans} resulted in a statistically significant increase of growth delays than *nsCRISPRi*^{trans} control in all the three media for most of the MER concentrations tested ($p < 0.05$, t-test) (Figs. 4b and 5a, b). Strains in M9 showed the largest recovery time for sub-lethal MER concentrations (11 h for MER = 1 μg/ml), representing a much higher delay than the same strains in MH and LB (maximum delay below 4 h).

Similarly, growth inhibition data for the *mcr-1* strains showed a 4-fold lower MIC in M9 (2 μg/ml and 1 μg/ml of COL for *nsCRISPRi*^{trans} and *sCRISPRi*^{trans}, respectively) than in rich MH and LB media (8 μg/ml and 4 μg/ml of COL for *nsCRISPRi*^{trans} and *sCRISPRi*^{trans}, respectively) (Figs. 4c and 5c and d). At sub-lethal COL levels, CRISPRi increased the delay up to 2 h (M9 at COL = 0.5 μg/ml) and 3 h (LB at COL = 2 μg/ml) with statistically significant differences from the *nsCRISPRi* control ($p < 0.05$, t-test) (Fig. 5b, c).

◀**Fig. 4**. Antibiotic re-sensitization of four *E. coli* clinical isolates grown in Mueller Hinton broth. **(a)** Illustration of the experimental setup involving four clinical isolates used as CRISPRi target strains. For each isolate, two conjugations were performed to deliver a CRISPRi array transcribing a targeting or non-targeting gRNA, generating the respective transconjugants with specific (*sCRISPRi*^{trans}) and non-specific (*nsCRISPRi*^{trans}) CRISPRi arrays. Transconjugant strains were tested in liquid Mueller Hinton (MH) broth in microplate assays. **(b–e)** Growth profiles and delays of *nsCRISPRi*^{trans} (subpanel on the middle left) and *sCRISPRi*^{trans} (subpanels on the middle right) from microplate assays to investigate meropenem (**b**), colistin (**c**) and cefotaxime (**d, e**) re-sensitization. *sCRISPRi*^{trans} were engineered with a one-plasmid CRISPRi platform, including HSL-inducible dCas9 and IPTG-inducible CRISPRi arrays targeting the bla_{NDM-5} (**b**), *mcr-1* (**c**), $bla_{ctx-M-14}$ (**d**) or $bla_{ctx-M-15}$ (**e**) gene. The overlapped curves in which a complete growth inhibition was achieved are indicated with an arrow, with the list of the corresponding antibiotic concentrations. Representative curves are shown from a set of at least two independent experiments. Growth delays (Δt) of treated strains relative to the growth profile without antibiotics are shown for *nsCRISPRi*^{trans} and *sCRISPRi*^{trans}. Bars represent the mean of two independent replicates with error bars indicating standard deviations and asterisks indicating statistical significance between the delay values of *nsCRISPRi*^{trans} and *sCRISPRi*^{trans} strains (t-test; *, $p < 0.05$; **, $p < 0.01$; ***, $p < 0.001$). The bars over the interrupted axis indicate the antibiotic concentration (MIC) for which OD_{600} was lower than 0.1. All the data come from experiments in MH media in the presence of IPTG and HSL. M-cr^{CI}_{arAT}, C-cr^{CI}_{arAT}, X14-$cr^{CI}_{arM(wt)}$, X15-$cr^{CI}_{arM(wt)}$ were used as *nsCRISPRi*^{trans} to investigate meropenem, colistin and cefotaxime re-sensitization. M-$cr^{CI}_{arM(wt)}$, C-$cr^{CI}_{arM1C1,}$ X14-$cr^{CI}_{arX14,}$ X15-cr^{CI}_{arX15} were used as *sCRISPRi*^{trans} to investigate meropenem, colistin and cefotaxime re-sensitization.

Results of growth inhibition assays with *ctx-M*-strains were consistent with previous observations: 24 h time course experiments performed in LB and MH media generated comparable outcomes in terms of MICs and growth delays, and all the tested strains showed a much higher increase in CTX-sensitivity when grown in M9 medium (Figs. 4d, e and 5e–h).

In particular, the results of *ctx-M-14* inhibition in M9 media (Fig. 5f) resembled those observed in MH (Fig. 4d), since a MIC (32 µg/ml) could be determined only for the strain bearing the specific CRISPRi, eventually resulting in a > 2-fold improvement of CTX-sensitivity compared with the control. As in MH, the effect of CRISPRi silencing in M9 was detectable as a significant increase in the recovery time of *sCRISPRi*^{trans} compared with its control, with the highest difference at CTX = 8 µg/ml (5.5 h) (Fig. 5f). Conversely, the two *ctx-M-14* strains in LB medium displayed the same MIC (512 µg/ml) and growth delays showed differences only up to 1 h (Fig. 5e). Despite the difference between both strains being statistically significant for CTX in the range 32–128 µg/ml ($p < 0.05$, t-test), a less effective re-sensitization for *ctx-M-14* was achieved in LB than in MH and M9. It may be caused by a weaker efficiency of the CRISPRi system in this strain due to the presence of an additional non-targeted β-lactamase and/or by a faster recovery of antibiotic-inhibited survivors in this medium condition.

Considering *ctx-M-15* strains, we found that the growth inhibition assays performed in LB prevent the determination of MIC values among the CTX concentration tested (Fig. 5g), as already observed in MH (Fig. 4e). However, CRISPRi repression on the *ctx-M-15* still promoted increased sensitivity to CTX in M9 medium, in which the MIC of *sCRISPRi*^{trans} was decreased by > 2-fold (32 µg/ml) (Fig. 5h). Moreover, growth profiles showed a significant increase of growth delay values from *nsCRISPRi*^{trans} to *sCRISPRi*^{trans}, with statistically significant differences for nearly all the CTX concentrations tested ($p < 0.05$, t-test) and values up to 5.5, 4.5 and 7 h in MH, M9 and LB, respectively (Fig. 5e, g, h).

Finally, to comprehensively assess the impact of growth conditions on CRISPRi efficiency, we tested cefotaxime re-sensitization in human urine (HU, purchased from BioIVT) using *ctx-M-15* transconjugants, consistent with the original source of the clinical sample as the NILS56 parental strain was collected from urine. As expected, both *nsCRISPRi*^{trans} and *sCRISPRi*^{trans} were able to grow in HU, reaching lower cell densities than in the other laboratory media (Fig. 6). Comparing the growth delays of both strains, no relevant difference is observed up to CTX = 128 µg/ml. For higher CTX concentrations, the *nsCRISPRi*^{trans} is still able to recover despite showing increasing growth delays up to 15 h. Conversely, the *sCRISPRi*^{trans} strain is re-sensitized to cefotaxime with a MIC of 256 µg/ml (Fig. 6 and Supplementary Material Table S6), also demonstrating the efficiency of the proposed solution under a condition that mimics the host microenvironment.

Taken together, data on *E. coli* isolates demonstrated that our trans-conjugative CRISPRi platform could be transferred into clinically relevant pathogens, in which the sensitivity to three different antibiotics has been successfully increased. In particular, we noticed that antibiotic sensitivity increased as a function of nutrient composition of the growth media, as evidenced by the comparison between MIC values in minimal, i.e., M9, and rich media, i.e., MH and LB. However, we found that the MIC fold-changes between *nsCRISPRi*^{trans} and *sCRISPRi*^{trans} did not substantially differ in the tested media. These data demonstrated the robustness of our platform under different growth conditions since the magnitude of CRISPRi repression efficiency was conserved among three different experimental conditions. The only exception was represented by the CTX-M-15 producing strain, in which the contribution of CRISPRi in decreasing the MIC was only detectable in M9 medium and also in a host-mimicking medium. In addition to MIC determination, the analysis of the growth delays of the tested strains treated with sub-inhibitory antibiotic concentrations allowed us to enrich our understanding of the effective potential of the CRISPRi system, which was reflected in a statistically significant increase of the recovery time for *sCRISPRi*^{trans} strains with respect to their controls in almost all the tested conditions.

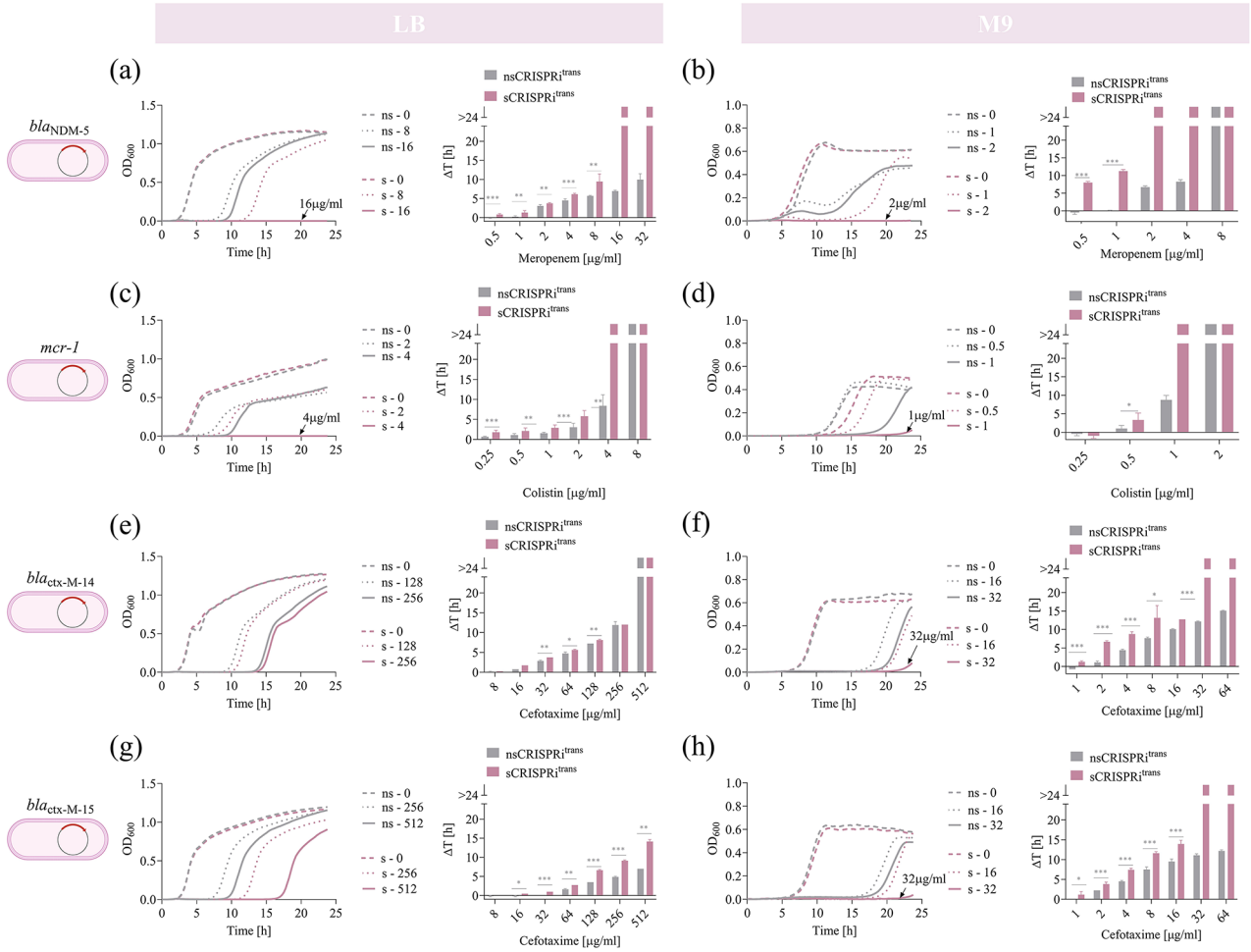

Fig. 5. Impact of growth media conditions on antibiotic re-sensitization of four *E. coli* clinical isolates grown in L-broth and minimal M9. **(a–h)** Growth profiles and delays of *nsCRISPRi*^{trans} and *sCRISPRi*^{trans} from microplate assays to investigate meropenem (**a, b**), colistin (**c, d**) and cefotaxime (**e–h**) re-sensitization. *sCRISPRi*^{trans} are engineered with the one-plasmid CRISPRi platform described in Fig. 4. Data in panels (**a, c, e, g**) were obtained from microplate assays in LB medium, and data in panels (**b, d,f, h**) were obtained from microplate assays in minimal M9 medium. Growth profiles are reported as representative curves from a set of at least three independent experiments. The growth curves of *nsCRISPRi*^{trans} and *sCRISPRi*^{trans} strains are overlapped in the same subpanels, as indicated in the legend. Only a subset of antibiotic concentrations is shown as growth profiles, while a complete set of growth curves is reported in Supplementary Material Figure S20. Growth delays (Δt) of treated strains relative to the growth profile without antibiotics are shown for *nsCRISPRi*^{trans} and *sCRISPRi*^{trans}. Bars represent the mean of at least three independent replicates with error bars indicating standard deviations and asterisks indicating statistical significance between the delay value of *nsCRISPRi*^{trans} and *sCRISPRi*^{trans} (t-test; *, $p < 0.05$; **, $p < 0.01$; ***, $p < 0.001$). The bars over the interrupted axis indicate the antibiotic concentration (MIC) for which OD_{600} was lower than 0.1. Data come from experiments in LB medium in the presence of IPTG and HSL, or M9 medium with lactose in the presence of HSL. Strains used to investigate meropenem, colistin and cefotaxime re-sensitization are listed in the caption of Fig. 4.

Discussion

The reversion of antibiotic resistance is one of the innovative approaches conceived to counteract multidrug-resistant pathogens and the slow pace in developing new antimicrobial drugs. We contributed to this goal by designing, testing and optimizing a CRISPRi platform for antibiotic re-sensitization in *E. coli*. In addition to previous studies, we quantified platform performance across several conditions, as bacteria can grow in different environments and adapt to many ecological niches, showing complex responses to antibiotic exposure. We spanned diverse experimental setups (e.g., liquid/solid media), growth conditions (minimal/rich laboratory media and host-mimicking media), protocols (dynamic growth in plate reader or in static incubator), and strains expressing ARGs with different mechanisms. Among them, we tested clinically relevant scenarios, e.g., four MDR isolates and growth media mimicking the host environment.

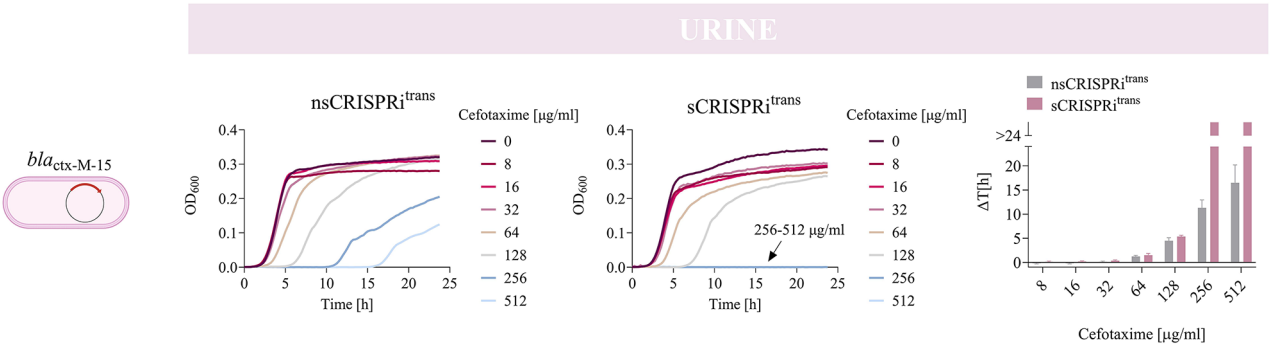

Fig. 6. Antibiotic re-sensitization of the $bla_{ctx-M-15}$ clinical isolate in human urine media. Growth profiles of transconjugants with specific (*sCRISPRi^{trans}*) and non-specific (*nsCRISPRi^{trans}*) CRISPRi arrays. Strains are engineered with a one-plasmid CRISPRi platform, including HSL-inducible dCas9 and IPTG-inducible CRISPRi array targeting the $bla_{ctx-M-15}$ gene (*sCRISPRi*) or with a non-targeting gRNA (*nsCRISPRi*). The overlapped curves in which a complete growth inhibition was achieved are indicated with an arrow, with the list of the corresponding antibiotic concentrations. Representative curves are shown from a set of three independent experiments. Growth delays (Δt) of treated strains relative to the growth profile without antibiotics are shown on the right for *nsCRISPRi^{trans}* and *sCRISPRi^{trans}*. Bars represent the mean of three independent replicates with error bars indicating standard deviations. The bars over the interrupted axis indicate the antibiotic concentration (MIC) for which OD_{600} was lower than 0.1. All the data come from experiments in human urine media in the presence of IPTG and HSL. The X15-cr$^{CI}_{arM(wt)}$ and X15-cr$^{CI}_{arX15}$ strains were used as *nsCRISPRi^{trans}* and *sCRISPRi^{trans}*, respectively, to investigate cefotaxime re-sensitization.

We demonstrated that our CRISPRi platform successfully increased the sensitivity to all the tested antibiotics, including last-resort drugs. However, we observed that re-sensitization was quantitatively variable and dependent on different factors such as strains, media and growth conditions. In particular, starting from laboratory strains, we measured a stronger re-sensitization capability in TOP10 F' than MG1655, which may be due to different physiological factors, e.g., antibiotic sensitivity of the background hosts, growth rate, expression levels of dCas9 and gRNA, or plasmid copy numbers. Second, results with clinical isolates showed that in standard M9 media the sensitivity to meropenem, colistin and cefotaxime was increased by 2- to >4-fold compared with rich media (MH and LB). In MH and LB we observed a higher variability both in terms of CRISPRi re-sensitization capability and resistance levels, as demonstrated by the overall increase of MICs. Importantly, re-sensitization was also confirmed in urine medium, used to mimic the environment from which the *E. coli* NILS56 strain was isolated. These results pave the way for a promising application of our CRISPRi platform for *in vitro* and potentially *in vivo* studies, but they also anticipate the importance of testing the robustness of the proposed solution under different conditions resembling the host environment.

Going further, a number of overarching limitations, not explicitly addressed in this study, still need to be solved to properly evaluate the applicability of our platform. For example, in the context of CRISPRi delivery, we adopted a broad host range conjugative system to enable the transfer of our platform in diverse bacteria. However, more studies are needed to evaluate its transfer to target bacteria other than *E. coli* and to test whether conjugation efficiency can be improved to reach clinically relevant efficiencies. Transferability to other species will also require a tuning of the regulatory parts for expressing dCas9 and CRISPRi array, depending on the target hosts. Regarding ARG targeting, it can be predictably expanded to cover different antibiotic resistance mechanisms, as CRISPRi only requires the design of short guide RNAs. In parallel, efforts are needed to broaden the characterization to other growth media, also including specific molecules known to affect antibiotic resistance response and development (e.g., metal ions)[58,59].

To overcome a potential source of therapeutic failure, the escape strategies of target strains must be fully understood and addressed. In this study we evaluated the CRISPRi capability to overcome mutations in the ARGs, which is extremely important to limit the emergence of new ARG variants. However, collective antibiotic tolerance mechanisms or escape mutations in CRISPRi circuit and strain genome can still occur. Mutations in CRISPRi circuits, herein studied, could be limited by the design of multi-targeting systems for the same gene or different *loci*, including both ARGs and ACR genes. Multiplexed targeting was demonstrated in this work by CRISPRi arrays showing no decreased efficiency compared with individual gRNAs against ARGs in medium-copy plasmids. The use of orthogonal dCas9 variants may provide further redundancy in the CRISPRi circuitry to retard the emergence of escape mutants[60]. More in-depth investigations on escapers may include the determination of other indexes like the mutant prevention concentration (MPC), to identify rare subpopulations evading antimicrobial action[61]. Such aspect is translationally crucial to design therapeutic strategies avoiding sub-inhibitory antibiotic concentrations, and to understand the full spectrum of mutations leading to AMR, including low-frequency genomic changes.

The presented data confirm the complex interplay between genetic and environmental factors contributing to AMR in bacteria. In this direction, thanks to the one-plasmid broad-host range design, our platform represents a readily usable tool to dissect AMR in *E. coli* and related species by perturbing the expression of specific genes (PBPs, porins, efflux pumps, etc.) individually or in combination.

Although some limitations still exist in applying this technology as a viable therapeutic, the work herein presented laid the foundations for further investigating the potential of CRISPRi in the global race against antibiotic resistance.

Materials and methods

Strains and plasmids

The strains used in this work are listed in Supplementary Material Table S1, while their plasmids and scope are detailed in Supplementary Material Table S2. Most of them are derivatives of the TOP10 F' parent strain with the F' episome conferring tetracycline resistance by the *tetA* gene, and overexpressing the LacI repressor via the $lacI^q$ locus. Exceptions are: the TOP10 strain with no F' plasmid that was used as a tetracycline sensitive control; the DH10B strain that was used as a donor chassis for conjugation assays; the model K-12 strain MG1655 that was used to test the performance of our system in another model strain; and the *E. coli* clinical isolates that were used as recipient strains. The bla_{NDM-5}, *mcr-1*, $bla_{ctx-M-14}$ and $bla_{ctx-M-15}$ clinical isolates correspond to the ECO167624, Lecco-02-EC08, NILS18 and NILS56 strains, respectively[48–50]. All the strains were long-term stored at – 80 °C in 20% glycerol stocks.

The pI13521 plasmid[39], based on the pSB1A2 backbone with the mutated pMB1 origin conferring high-copy vector maintenance per cell, was used as the ampicillin resistance plasmid. It constitutively expresses $bla_{TEM-116}$, coding for a β-lactamase, by the P_{bla} promoter.

The pJ107202 plasmid[39], based on the medium-copy kanamycin-resistant pSB3K3 backbone with the p15A origin, was used as a constitutive source of dCas9, via an expression cassette driven by the weak P_{J23116} promoter.

The pGDP1 NDM-1 and pGDP2 MCR-1[47] plasmids were gifts from Gerard Wright (Addgene plasmids #112883 and #118404). They were used as constitutive expression vectors for a codon-optimized bla_{NDM-1} (by the P_{bla} promoter) and *mcr-1* (by the P_{lac} promoter), respectively. Both plasmids have a kanamycin resistance gene and are replicated at medium-copy number via the pBR322 origin.

The pTA-mob plasmid[53] was a gift from Rahmi Lale (NTNU). This helper plasmid includes a gentamicin resistance marker, a pBBR1 broad-host range replicon conferring medium-copy maintenance, and provides *in trans* all the genes necessary for conjugative transfer of mobilizable plasmids that have an origin of transfer (oriT). Recognition of the oriT sequence by the relaxase expressed *in trans* from pTA-Mob allowed the CRISPRi-vector to be transferred into antibiotic-resistant recipient cells, which become stable transconjugants.

The chloramphenicol-resistant low-copy pSB4C5 backbone[39], having the pSC101 origin, was adopted for cloning, heterologous expression of synthetic circuits (P_{LlacO1}-driven sgRNAs or CRISPRi arrays, P_{lux}-driven dCas9 in HSL-inducible dCas9 circuits), and as a mobilizable plasmid using the oriT sequence, amplified from the RK2 plasmid (ATCC 37125)[62].

Reagents and media

Isopropyl-β-D-1-thiogalactopyranoside (IPTG, #I1284, Sigma Aldrich) and N-3-oxohexanoyl-L-homoserine lactone (HSL, #K3007, Sigma Aldrich), routinely stored at -20 °C, were used as chemical inducers of recombinant gene expression for RNA guides (sgRNAs or CRISPRi arrays) and for dCas9 in the circuit architectures with inducible dCas9, respectively. Ampicillin (AMP, 100 mg/ml), kanamycin (KAN, 50 mg/ml), chloramphenicol (CHL, 34 mg/ml), gentamicin (GM, 50 mg/ml), tetracycline (TC, 5 mg/ml) stocks were routinely stored at – 20 °C. The powders of levofloxacin (LEV), ciprofloxacin (CIP), meropenem (MER), colistin (COL) and cefotaxime (CTX) were stored at – 20 °C and used to make fresh stocks at every use. Antibiotic powders were dissolved in deionized water except chloramphenicol (ethanol) and meropenem (deionized water with 10.4 mg/ml of sodium carbonate). All of them were filter-sterilized (0.2 µm) before storage. Meropenem and colistin agar plates were used within two days from preparation.

Unless differently indicated, L-broth (LB; 10 g/L tryptone, 5 g/L yeast extract, 10 g/L sodium chloride) was used as a medium for cloning and quantitative experiments. Agar plates were prepared by adding 15 g/L agar to the liquid medium before autoclaving. Mueller Hinton (MH) and M9 (M9 salts 11.28 g/L, $MgSO_4$ 2 mM, $CaCl_2$ 0.1 mM, and 0.1% lactose as carbon source) were used as liquid media in the experiments with clinical isolates. Tween 20 0.1% was added to M9 medium in experiments with the X14-$cr^{CI}_{arM(wt)}$, X14-cr^{CI}_{arX14}, X15-$cr^{CI}_{arM(wt)}$, and X15-cr^{CI}_{arX15} strains (Supplementary Material Table S1).

Selective media refers to medium only including the antibiotics needed for plasmid maintenance or strain selection (without the target antibiotic tested for growth inhibition): chloramphenicol (12.5 µg/ml), kanamycin (25 µg/ml), gentamicin (20 µg/ml), levofloxacin (2 µg/ml) and ciprofloxacin (2 µg/ml), according to the specific plasmids. Antibiotics tested for growth inhibition were ampicillin, tetracycline, meropenem, colistin and cefotaxime, added at the indicated concentrations.

Circuit assembly

Unless differently indicated, the BioBrick Standard Assembly procedure[63] was adopted for plasmid construction, enabling binary assembly steps that left a standard DNA junction (TACTAGAG) between the joint parts. The dCas9 expression systems and the sgRNA scaffold, with synthetic tetraloop for the expression of the gRNA:tracrRNA as a unique molecule, were obtained previously[39], the oriT sequence was PCR-amplified from RK2 and all the CRISPRi arrays were obtained by *de novo* DNA synthesis (GenScript, Piscataway, NJ, USA). Digestions with *EcoRI* and *SpeI* restriction sites in DNA parts with dCas9 and CRISPRi array, respectively, were avoided, due to illegal restriction sites in their sequences but their assembly was still possible with BioBrick restriction enzymes (*XbaI* and *PstI*).

sgRNA cassettes were customized by changing the 20-nt targeting region via mutagenesis with divergent primers, using PCR amplification, *DpnI* digestion, T4 polynucleotide kinase and ligase reactions, as previously carried out[39]. Targeting regions were designed via the Benchling CRISPR tool (https://benchling.com) by setting

a 20-nt (for sgRNAs) or 30-nt (for CRISPRi arrays) guide length, GCA_00005845.2 reference genome, and the optimized score by Doench et al.[64]. Each sgRNA cassette was designed with its own IPTG-inducible P_{LlacO1} promoter.

DNA purification kits (Macherey-Nagel), restriction enzymes, T4 DNA ligase and T4 polynucleotide kinase (Thermo Scientific), Antarctic phosphatase (New England BioLabs), and Phusion Hot Start II PCR kit (Thermo Scientific) were used according to manufacturer's indications. Sequencing and oligonucleotides synthesis services were from Eurofins Genomics Germany GmbH.

Growth inhibition assays

Strains from long-term stocks were streaked on an LB agar plate and incubated overnight (14–16 h) at 37 °C.

For tests with laboratory strains, single colonies ($N=3$) were used to inoculate 0.5 ml of selective media in 2-ml tubes and cultures were grown overnight at 37 °C, 220 rpm in an orbital shaker. The grown cultures were 100-fold diluted in 200 µl of selective LB in a 96-well microplate, in which we added IPTG (500 µM) and HSL (10 nM, unless differently indicated) to trigger guide RNAs and dCas9 expression, as required, and antibiotics were added to reach the desired concentrations. The 96-well plate was incubated at 37 °C in an Infinite F200Pro reader (Tecan) and assayed for 24 h via an automated sampling program (i-control software, Tecan): linear shaking (5 s, 3-mm amplitude), 5 s wait, absorbance measurement (600 nm), 5-min sampling time.

For tests involving clinical isolates, strains were grown as previously described[65] to start experiments with exponentially growing cells at comparable densities. Briefly, colonies were used to inoculate 2 ml of selective media in 50-ml tubes and cultures ($N=3$) were grown overnight at 37 °C, 200 rpm in an orbital shaker. The overnight cultures were diluted to 0.05 OD_{600} in fresh media and incubated for 3–4 h under the same conditions as above. These cultures were finally diluted to 0.0005 OD_{600} in 200 µl of the indicated medium in a 96-well microplate, in which IPTG (500 µM), HSL (10 nM), and the required antibiotics were added to reach the desired concentrations. IPTG was omitted when using M9 media with lactose, which already activates the P_{LlacO1} promoter. The microplate was assayed as previously described[65] at 37 °C in a Spark reader (Tecan) for 24 h via the following kinetic cycle programmed with Spark Control v.2.2 software (Tecan): linear shaking (30 s, 5 mm), orbital shaking (30 s, 5 mm), 30 s wait, absorbance measurement (600 nm), 60-s wait, linear shaking (120 s, 5 mm), 30 s wait, orbital shaking (120 s, 5 mm), 30 s wait, orbital shaking (60 s, 5 mm), 15-min sampling time. Sterile media without bacteria was also included to measure the absorbance background.

Occasionally, at the end of experiments with ampicillin and meropenem, 3 µl of bacteria-free supernatants from cultures grown in different wells were applied on non-selective LB agar plates on which an AMP- or MER-sensitive strain was previously plated. The plates were incubated overnight at 37 °C and inhibition halos were observed, qualitatively indicating antibiotic activity and, consequently, its degradation due to the β-lactamase enzymes released in the media.

For clinical isolate strains, growth inhibition was also measured according to EUCAST guidelines by broth microdilution assays[66]. Briefly, overnight cultures grown in cation-adjusted MH broth in the presence of IPTG (500 µM) and HSL (10 nM) were diluted in 200 µl of the same medium to obtain a bacterial density of $5*10^5$ cells per ml (based on an OD_{600} to CFU/ml calibration curve, data not shown) in a 96-well microplate. The microplate was incubated statically at 35 °C for 16 h.

Growth inhibition assays on solid media were carried out by plating serial dilutions of the recombinant cultures ($N=2$) grown overnight in the 2-ml tubes. LB and MH plates were supplemented with the antibiotics required for ARG-bearing plasmid selection, IPTG (500 µM) and HSL (10 nM, unless differently stated) as required, and the target antibiotic (ampicillin, tetracycline, meropenem or colistin) at different concentrations. Plates were incubated at 37 °C overnight.

In all the experiments, antibiotics (CHL and KAN, when required) were added to solid and liquid media during the overnight growth steps before the assays for the selection of strains with the CRISPRi system. No other antibiotics were added for the maintenance of ARG-bearing plasmids, for which no loss was observed during strain propagation (data not shown).

Escaper analysis

At the end of the 24-h growth assays in 96-well microplates, escaper cultures recovering from one of the highest antibiotic concentrations were streaked on selective LB agar without target antibiotic and incubated overnight at 37 °C. From each plate, one colony was used to inoculate 5 ml of selective LB, incubated overnight at 37 °C, 220 rpm. The grown cultures were 100-fold diluted in a microplate to run a second-round microplate assay under the same conditions as the first round microplate assay that originated the escaper culture. The rest of the culture was used to extract plasmid DNA. Plasmids were used to identify mutations by sequencing with primers covering guide RNAs, dCas9 and ARG target site (Supplementary Material Table S3), and restriction mapping on 1% agarose gel electrophoresis.

Conjugation

Donor and recipient strains from a streaked agar plate were used to inoculate 5 ml of selective media and grown overnight at 37 °C, 220 rpm. Cultures were 100-fold diluted and incubated under the same conditions until they reached 0.25 OD_{600}. Then, 1 ml was withdrawn from each tube, gently spun down (3000 rpm, 5 min) and washed twice with sterile PBS to remove residual antibiotics from the cultures. OD_{600} was again measured and each culture was concentrated to reach a final OD_{600} of 0.5. Mating pairs were then combined in a 1:1 donor:recipient ratio and 100 µl of the mixture was pipetted on a non-selective rich media agar plate (LB or MH) that was further incubated at 37 °C for 20 h. The conjugation mixture was scraped up from the plate and transferred into 1 ml PBS in a 1.5-ml tube. Conjugation was interrupted by vortexing, centrifuging (5000 rpm, 3 min) and resuspending the mating mixture in PBS, which was finally diluted as appropriate. Protocol definition was based

on a screening of different parameters that maximized conjugation frequency, i.e., bacterial density, growth phase, solid vs. liquid media, strains ratio, and size of the spotted mixture (data not shown).

For conjugation of the M-res, C-res, M-res^{CI}, C-res^{CI} strains, the mating mixture was then plated on agar media (LB for M-res and C-res; MH for M-res^{CI} and C-res^{CI}) with CHL + auxiliary antibiotic (i.e., KAN, LEV or CIP, as required to select ARG-bearing plasmids - see Supplementary Material Table S1) to select for transconjugants; the same mixture was plated on media to select for recipients (auxiliary antibiotic), and survivors (CHL + IPTG/HSL + target antibiotic, i.e., MER or COL).

For conjugation of A-res, having no auxiliary antibiotic in the ARG-bearing plasmid, the grown mixture was then plated on LB agar with CHL + AMP to select for transconjugants, AMP to select for recipients, and CHL + AMP + IPTG/HSL to select for survivors to antibiotic treatment. The absence of $bla_{TEM-116}$ inhibition when dCas9 and sgRNA were not expressed was confirmed by colony counts with and without AMP (data not shown).

For conjugation of the X14-res^{CI}, X15-res^{CI} strains, for which no auxiliary antibiotics were exploited, the mixture was plated on minimal M9 plates with 0.4% lactose with CHL to select for transconjugants (the DH10B-based donor was unable to grow in minimal media without leucine and was also unable to consume lactose), and on the same agar media without CHL to select for recipients.

In all cases, plates were incubated overnight at 37 °C. For all the clinical isolates, transconjugant colonies were cultured and used for further characterization in liquid media via microplate assays and broth microdilution assays according to the EUCAST protocol. When indicated, the colony forming units (CFUs) for transconjugants, recipients and survivors were quantified as N_T, N_R and N_S, respectively. These CFU values were used to calculate conjugation efficiency (E_{conj}), as N_T/N_R, and the proportion of re-sensitized transconjugants, as $1\text{-}N_S/N_T$. Unless differently indicated, three independent experiments were performed for each condition.

Data analysis

For each sample in microplate assays, raw absorbance time series was background-subtracted using the raw measurement of sterile media, obtaining an OD_{600} time series that is proportional to bacterial density. The linearity of the plate reader was assessed up to OD_{600} values of 0.7.

The minimum inhibitory concentration (MIC) in microplate assays was determined as the antibiotic concentration for which cell growth is maintained lower than OD_{600} 0.1 over 24 h. The minimum inhibitory concentration was also measured for EUCAST broth microdilution assays, as the lowest antibiotic concentration in which no bacterial growth was detected. To distinguish this index from the MIC obtained from dynamic microplate assays, this value is referred to as EUCAST MIC.

Growth profiles of strains in microplate assays at different antibiotic concentrations were used to quantify the CRISPRi-mediated antibiotic re-sensitization by calculating $\Delta t = t_{0.1,AB+} - t_{0.1,AB-}$, where $t_{0.1,AB+}$ and $t_{0.1,AB-}$ are the time points in which the cultures with and without the tested antibiotic reach $OD_{600} = 0.1$. This index was computed for each antibiotic concentration within a biological replicate, for which the initial density in the microplate is expected to be the same since the wells were inoculated with the same pre-culture.

IC_{99} was determined in agar plate assays as the antibiotic concentration inhibiting 99% of the bacterial growth, measured as colony count, compared with the plate in the absence of the target antibiotic.

Statistical tests were carried out using Matlab R2017b (MathWorks) or Microsoft Excel to compare mean values of growth delay across different strains for each antibiotic concentration tested. Unpaired one-sided t-test was used to compare resistant and CRISPRi strains. Two-way ANOVA with replicates was used to compare circuit architectures, with dCas9 (constitutive vs. inducible) and guide RNA (double sgRNA vs. CRISPRi array) as main factors. One-way ANOVA was used to compare circuit architectures including gNDM1. A p-value of 0.05 was used as a cutoff for statistical significance. Graphs were generated using GraphPad Prism 8.3.0.

Data availability

The data that support the findings of this study are available from the corresponding author upon request.

Received: 31 July 2024; Accepted: 2 December 2024
Published online: 02 January 2025

References

1. 2021 antibacterial agents in clinical and preclinical development: an overview and analysis (2024, accessed 2 Apr 2024). https://www.who.int/publications-detail-redirect/9789240047655.
2. Butler, M. S., Henderson, I. R., Capon, R. J. & Blaskovich, M. A. T. Antibiotics in the clinical pipeline as of December 2022. *J. Antibiot. (Tokyo)*. **76**(8), 431–473. https://doi.org/10.1038/s41429-023-00629-8 (2023).
3. Hwang, I. Y. et al. Engineered probiotic *Escherichia coli* can eliminate and prevent *Pseudomonas aeruginosa* Gut infection in animal models. *Nat. Commun.* **8**(1), 15028. https://doi.org/10.1038/ncomms15028 (2017).
4. Theuretzbacher, U. & Piddock, L. J. V. Non-traditional antibacterial therapeutic options and challenges. *Cell. Host Microbe*. **26**(1), 61–72. https://doi.org/10.1016/j.chom.2019.06.004 (2019).
5. Kiga, K. et al. Development of CRISPR-Cas13a-based antimicrobials capable of sequence-specific killing of target bacteria. *Nat. Commun.* **11**(1), 2934. https://doi.org/10.1038/s41467-020-16731-6 (2020).
6. Peters, J. M. et al. Enabling genetic analysis of diverse bacteria with mobile-CRISPRi. *Nat. Microbiol.* **4**(2), 244–250. https://doi.org/10.1038/s41564-018-0327-z (2019).
7. McNeil, M. B. & Cook, G. M. Utilization of CRISPR Interference to validate MmpL3 as a drug target in *Mycobacterium tuberculosis*. *Antimicrob. Agents Chemother.* **63**, 8. https://doi.org/10.1128/AAC.00629-19 (2019).
8. Yasir, M. et al. TraDIS-Xpress: a high-resolution whole-genome assay identifies novel mechanisms of Triclosan Action and Resistance. *Genome Res.* **30**(2), 239–249. https://doi.org/10.1101/gr.254391.119 (2020).
9. Rousset, F. & Bikard, D. C. R. I. S. P. R. Screens in the era of microbiomes. *Curr. Opin. Microbiol.* **57**, 70–77. https://doi.org/10.1016/j.mib.2020.07.009 (2020).

10. Silvis, M. R. et al. Morphological and transcriptional responses to CRISPRi knockdown of essential genes in *Escherichia coli*. *mBio* **12**(5), e0256121. https://doi.org/10.1128/mBio.02561-21 (2021).
11. Bosch, B. et al. Genome-wide gene expression tuning reveals diverse vulnerabilities of *M. tuberculosis*. *Cell* **184**(17), 4579–4592e24. https://doi.org/10.1016/j.cell.2021.06.033. (2021).
12. Kurepina, N. et al. CRISPR inhibition of essential peptidoglycan biosynthesis genes in *Mycobacterium abscessus* and its impact on β-Lactam susceptibility. *Antimicrob. Agents Chemother.* **66**(4), e0009322. https://doi.org/10.1128/aac.00093-22 (2022).
13. Nguyen, T. Q. et al. Interference-based inhibition of MAB_0055c expression alters drug sensitivity in *Mycobacterium abscessus*. *Microbiol. Spectr.* **11**(3), e0063123. https://doi.org/10.1128/spectrum.00631-23 (2023).
14. Bikard, D. et al. Exploiting CRISPR-Cas nucleases to produce sequence-specific antimicrobials. *Nat. Biotechnol.* **32**(11), 1146–1150. https://doi.org/10.1038/nbt.3043 (2014).
15. Citorik, R. J., Mimee, M. & Lu, T. K. Sequence-specific antimicrobials using efficiently delivered RNA-Guided nucleases. *Nat. Biotechnol.* **32**(11), 1141–1145. https://doi.org/10.1038/nbt.3011 (2014).
16. Rodrigues, M., McBride, S. W., Hullahalli, K., Palmer, K. L. & Duerkop, B. A. Conjugative delivery of CRISPR-Cas9 for the selective depletion of antibiotic-resistant *Enterococci*. *Antimicrob. Agents Chemother.* **63**, 11. https://doi.org/10.1128/AAC.01454-19 (2019).
17. Selle, K. et al. In vivo targeting of *Clostridioides difficile* using phage-delivered CRISPR-Cas3 antimicrobials. *mBio* **11**, 2. https://doi.org/10.1128/mBio.00019-20 (2020).
18. Mayorga-Ramos, A., Zúñiga-Miranda, J., Carrera-Pacheco, S. E., Barba-Ostria, C. & Guamán, L. P. CRISPR-Cas-based antimicrobials: design, challenges, and bacterial mechanisms of resistance. *ACS Infect. Dis.* **9**(7), 1283–1302. https://doi.org/10.1021/acsinfecdis.2c00649 (2023).
19. Yosef, I., Manor, M., Kiro, R. & Qimron, U. Temperate and lytic bacteriophages programmed to sensitize and kill antibiotic-resistant bacteria. *Proc. Natl. Acad. Sci. U S A.* **112** (23), 7267–7272. https://doi.org/10.1073/pnas.1500107112 (2015).
20. Hamilton, T. A. et al. Efficient inter-species conjugative transfer of a CRISPR nuclease for targeted bacterial killing. *Nat. Commun.* **10**(1), 4544. https://doi.org/10.1038/s41467-019-12448-3 (2019).
21. Reuter, A. et al. Plasmids (TAPs) combining conjugation and CRISPR/Cas systems achieve strain-specific antibacterial activity. *Nucleic Acids Res.* **49**(6), 3584–3598. https://doi.org/10.1093/nar/gkab126 (2021).
22. Neil, K. et al. High-efficiency delivery of CRISPR-Cas9 by engineered probiotics enables precise microbiome editing. *Mol. Syst. Biol.* **17**(10), e10335. https://doi.org/10.15252/msb.202110335 (2021).
23. Mc Ginty, S. E., Rankin, D. J. & Brown, S. P. Horizontal gene transfer and the evolution of bacterial cooperation. *Evol. Int. J. Org. Evol.* **65**(1), 21–32. https://doi.org/10.1111/j.1558-5646.2010.01121.x (2011).
24. Cui, L. & Bikard, D. Consequences of Cas9 cleavage in the chromosome of *Escherichia coli*. *Nucleic Acids Res.* **44**(9), 4243–4251. https://doi.org/10.1093/nar/gkw223 (2016).
25. Wang, P. et al. Eliminating Mcr-1-Harbouring plasmids in clinical isolates using the CRISPR/Cas9 system. *J. Antimicrob. Chemother.* **74**(9), 2559–2565. https://doi.org/10.1093/jac/dkz246 (2019).
26. Uribe, R. V. et al. Bacterial resistance to CRISPR-Cas antimicrobials. *Sci. Rep.* **11**(1), 17267. https://doi.org/10.1038/s41598-021-96735-4 (2021).
27. Botelho, J., Cazares, A. & Schulenburg, H. The ESKAPE mobilome contributes to the spread of antimicrobial resistance and CRISPR-mediated conflict between mobile genetic elements. *Nucleic Acids Res.* **51**(1), 236–252. https://doi.org/10.1093/nar/gkac1220 (2023).
28. Li, Q. et al. Improving the editing efficiency of CRISPR-Cas9 by reducing the generation of escapers based on the surviving mechanism. *ACS Synth. Biol.* **12**(3), 672–680. https://doi.org/10.1021/acssynbio.2c00619 (2023).
29. Qi, L. S. et al. Repurposing CRISPR as an RNA-Guided platform for sequence-specific control of gene expression. *Cell* **152**(5), 1173–1183. https://doi.org/10.1016/j.cell.2013.02.022 (2013).
30. Larson, M. H. et al. CRISPR interference (CRISPRi) for sequence-specific control of gene expression. *Nat. Protoc.* **8**(11), 2180–2196. https://doi.org/10.1038/nprot.2013.132 (2013).
31. Li, Q. et al. Engineering a CRISPR interference system to repress a class 1 Integron in *Escherichia coli*. *Antimicrob. Agents Chemother.* **64**, 3. https://doi.org/10.1128/AAC.01789-19 (2020).
32. Faulkner, V. et al. Re-sensitization of *Mycobacterium smegmatis* to rifampicin using CRISPR interference demonstrates its utility for the study of non-essential drug resistance traits. *Front. Microbiol.* **11**, 856. https://doi.org/10.3389/fmicb.2020.619427 (2020).
33. Wan, X. et al. Engineering a CRISPR interference system targeting AcrAB-TolC efflux pump to prevent multidrug resistance development in *Escherichia coli*. *J. Antimicrob. Chemother.* **77**(8), 2158–2166. https://doi.org/10.1093/jac/dkac166 (2022).
34. Wang, K. & Nicholaou, M. Suppression of antimicrobial resistance in MRSA using CRISPR-dCas9. *Am. Soc. Clin. Lab. Sci.* **30**(4), 207–213. https://doi.org/10.29074/ascls.30.4.207 (2017).
35. Yao, S. et al. Efficient suppression of natural plasmid-borne gene expression in Carbapenem-resistant *Klebsiella pneumoniae* using a compact CRISPR interference system. *Antimicrob. Agents Chemother.* **66**(11), e00890–e00822. https://doi.org/10.1128/aac.00890-22
36. Ward, R. D. et al. Essential gene knockdowns reveal genetic vulnerabilities and antibiotic sensitivities in acinetobacter baumannii. *mBio* **2023**, e02051-23. https://doi.org/10.1128/mbio.02051-23 (2023).
37. Lee, T. S. et al. BglBrick vectors and datasheets: a synthetic biology platform for gene expression. *J. Biol. Eng.* **5**(1), 12. https://doi.org/10.1186/1754-1611-5-12 (2011).
38. Shetty, R. P., Endy, D. & Knight, T. F. Engineering BioBrick vectors from BioBrick parts. *J. Biol. Eng.* **2**(1), 5. https://doi.org/10.1186/1754-1611-2-5 (2008).
39. Bellato, M. et al. CRISPR Interference modules as low-burden logic inverters in synthetic circuits. *Front. Bioeng. Biotechnol.* **9**, 743950. https://doi.org/10.3389/fbioe.2021.743950 (2022).
40. Schultz, D., Palmer, A. C. & Kishony, R. Regulatory dynamics determine cell Fate following abrupt antibiotic exposure. *Cell. Syst.* **5**(5), 509–517e3. https://doi.org/10.1016/j.cels.2017.10.002 (2017).
41. Meredith, H. R. et al. Applying ecological resistance and resilience to dissect bacterial antibiotic responses. *Sci. Adv.* **4**(12), eaau1873. https://doi.org/10.1126/sciadv.aau1873 (2018).
42. Jinek, M. et al. Programmable dual-RNA-Guided DNA endonuclease in adaptive bacterial immunity. *Science* **337**(6096), 816–821. https://doi.org/10.1126/science.1225829 (2012).
43. Reis, A. C. et al. Simultaneous repression of multiple bacterial genes using nonrepetitive extra-long sgRNA arrays. *Nat. Biotechnol.* **37**(11), 1294–1301. https://doi.org/10.1038/s41587-019-0286-9 (2019).
44. Ronda, C., Pedersen, L. E., Sommer, M. O. A. & Nielsen, A. T. CRMAGE: CRISPR optimized MAGE recombineering. *Sci. Rep.* **6**, 19452. https://doi.org/10.1038/srep19452 (2016).
45. Zhang, S. & Voigt, C. A. Engineered dCas9 with reduced toxicity in bacteria: implications for genetic circuit design. *Nucleic Acids Res.* **46**(20), 11115–11125. https://doi.org/10.1093/nar/gky884 (2018).
46. Huang, H. H. et al. dCas9 Regulator to neutralize competition in CRISPRi circuits. *Nat. Commun.* **12**(1), 1692. https://doi.org/10.1038/s41467-021-21772-6 (2021).
47. Cox, G. et al. A common platform for antibiotic dereplication and adjuvant discovery. *Cell. Chem. Biol.* **24**(1), 98–109. https://doi.org/10.1016/j.chembiol.2016.11.011 (2017).
48. Principe, L. et al. Multicenter prospective study on the prevalence of colistin resistance in *Escherichia coli*: relevance of Mcr-1-Positive clinical isolates in Lombardy, Northern Italy. *Infect. Drug Resist.* **11**, 377–385. https://doi.org/10.2147/IDR.S160489 (2018).

49. Batisti Biffignandi, G. et al. Genomic characterization of an O101:H9-ST167 NDM-5-producing *Escherichia coli* strain from a Kitten in Italy. *Microbiol. Spectr.* **10**(3), e0083222. https://doi.org/10.1128/spectrum.00832-22 (2022).
50. Bleibtreu, A. et al. The rpoS gene is predominantly inactivated during laboratory storage and undergoes source-sink evolution in *Escherichia coli* species. *J. Bacteriol.* **196**(24), 4276–4284. https://doi.org/10.1128/JB.01972-14 (2014).
51. Darby, E. M. A. et al. Molecular mechanisms of antibiotic resistance revisited. *Nat. Rev. Microbiol.* **21**(5), 280–295. https://doi.org/10.1038/s41579-022-00820-y (2023).
52. Qin, J. et al. A method for increasing electroporation competence of gram-negative clinical isolates by polymyxin B nonapeptide. *Sci. Rep.* **12**(1), 11629. https://doi.org/10.1038/s41598-022-15997-8 (2022).
53. Strand, T. A., Lale, R., Degnes, K. F., Lando, M. & Valla, S. A. New and improved host-independent plasmid system for RK2-Based conjugal transfer. *PLOS ONE* **9**(3), e90372. https://doi.org/10.1371/journal.pone.0090372 (2014).
54. Grönthal, T. et al. Sharing more than friendship—transmission of NDM-5 ST167 and CTX-M-9 ST69 *Escherichia coli* between dogs and humans in a family, Finland, 2015. *Eurosurveillance* **23**, 27. https://doi.org/10.2807/1560-7917.ES.2018.23.27.1700497 (2018).
55. Castanheira, M., Simner, P. J. & Bradford, P. A. Extended-spectrum β-Lactamases: an update on their characteristics, epidemiology and detection. *JAC-Antimicrob Resist.* **3**(3), dlab092. https://doi.org/10.1093/jacamr/dlab092 (2021).
56. Rana, C. et al. Global epidemiology of CTX-M-Type β-Lactam resistance in human and animal. *Comp. Immunol. Microbiol. Infect. Dis.* **86**, 101815. https://doi.org/10.1016/j.cimid.2022.101815 (2022).
57. Varik, V., Oliveira, S. R. A., Hauryliuk, V. & Tenson, T. Composition of the outgrowth medium modulates wake-up kinetics and ampicillin sensitivity of stringent and relaxed *Escherichia coli*. *Sci. Rep.* **6** (1), 22308. https://doi.org/10.1038/srep22308 (2016).
58. Hubeny, J. et al. Industrialization as a source of heavy metals and antibiotics which can enhance the antibiotic resistance in wastewater, sewage sludge and river water. *PloS One* **16**(6), e0252691. https://doi.org/10.1371/journal.pone.0252691 (2021).
59. Faure, M. E., Cilibrizzi, A., Abbate, V., Bruce, K. D. & Hider, R. C. Effect of iron chelation on anti-pseudomonal activity of doxycycline. *Int. J. Antimicrob. Agents*. **58**(6), 106438. https://doi.org/10.1016/j.ijantimicag.2021.106438 (2021).
60. De Marchi, D. et al. Design and model-driven analysis of synthetic circuits with the *Staphylococcus aureus* Dead-Cas9 (sadCas9) as a programmable transcriptional regulator in bacteria. *ACS Synth. Biol.* **13**(3), 763–780. https://doi.org/10.1021/acssynbio.3c00541 (2024).
61. Cantón, R. & Morosini, M. I. Emergence and spread of antibiotic resistance following exposure to antibiotics. *FEMS Microbiol. Rev.* **35**(5), 977–991. https://doi.org/10.1111/j.1574-6976.2011.00295.x (2011).
62. Meyer, R., Figurski, D. & Helinski, D. R. Molecular Vehicle properties of the broad host range plasmid RK2. *Science* **190**(4220), 1226–1228. https://doi.org/10.1126/science.1060178 (1975).
63. Knight, T. Idempotent vector design for standard assembly of Biobricks; Defense Technical Information Center. https://doi.org/10.21236/ADA457791 (2003).
64. Doench, J. G. et al. Optimized sgRNA Design to maximize activity and minimize off-Target effects of CRISPR-Cas9. *Nat. Biotechnol.* **34**(2), 184–191. https://doi.org/10.1038/nbt.3437 (2016).
65. Bertaux, F. et al. Enhancing bioreactor arrays for automated measurements and reactive control with ReacSight. *Nat. Commun.* **13**(1), 3363. https://doi.org/10.1038/s41467-022-31033-9 (2022).
66. eucast: EUCAST (2024, accessed Oct 31, 2024). https://www.eucast.org.

Acknowledgements

The authors want to thank Daniele Pastorelli, Melissa Spalla, Aseel Abu-Alshaar, Francesca Piscopiello (Univ. Pavia) and Viktoriia Gross (INRIA/Pasteur) for their help in experimental work with clinical isolates; Angelo Serafini, Mirko Martini and Marianna Caldarulo (Univ. Pavia) for their work with laboratory strains and preliminary work on protocol design; Maria Gabriella Cusella De Angelis (Univ. Pavia) for sharing lab space and instruments; Philippe Glaser (Pasteur) and Imane El Meouche (INSERM) for their help on strain characterization. This work was supported by Innovation HUB Regione Lombardia, Italy (grant 1139857), by Fondazione Cariparo, Italy (grant 59576, 2021) and by ANR, France (grant 20-PAMR-0001 Anoruti and 20-PAMR-0010 Seq2DiAg). Lorenzo Pasotti also acknowledges funding support from the INCEPTION visiting scientist fellowship (ANR, Investissements d'Avenir, France ANR-16-CONV-0005).

Author contributions

A.F.C., P.M. and L.P. conceived the study. A.F.C., A.P., R.M., G.B., P.M. and L.P. designed the experiments. A.F.C. constructed the plasmids. A.F.C. and M.C. conducted the quantitative experiments. A.F.C., M.B., G.B., P.M. and L.P. analyzed the data. A.F.C. and L.P. wrote the manuscript. M.B., G.B. and P.M. contributed to manuscript finalization. All authors read and approved the manuscript.

Competing interests

The authors declare no competing interests.

Additional information

Supplementary Information The online version contains supplementary material available at https://doi.org/10.1038/s41598-024-81989-5.

Correspondence and requests for materials should be addressed to L.P.